

# Nanoscale

Accepted Manuscript

This article can be cited before page numbers have been issued, to do this please use: S. Khorrami, A. Alifarsangi, L. J. Mohammed, A. M. Amshawee and A. Zarrabi, *Nanoscale*, 2026, DOI: 10.1039/D5NR04613K.



This is an Accepted Manuscript, which has been through the Royal Society of Chemistry peer review process and has been accepted for publication.

Accepted Manuscripts are published online shortly after acceptance, before technical editing, formatting and proof reading. Using this free service, authors can make their results available to the community, in citable form, before we publish the edited article. We will replace this Accepted Manuscript with the edited and formatted Advance Article as soon as it is available.

You can find more information about Accepted Manuscripts in the [Information for Authors](#).

Please note that technical editing may introduce minor changes to the text and/or graphics, which may alter content. The journal's standard [Terms & Conditions](#) and the [Ethical guidelines](#) still apply. In no event shall the Royal Society of Chemistry be held responsible for any errors or omissions in this Accepted Manuscript or any consequences arising from the use of any information it contains.

## Metal-based nanoparticles' potential in alzheimer's disease diagnosis, therapy and theranostics

Sadegh Khorrami<sup>1\*</sup>, Atena Alifarsangi<sup>2</sup>, Layth Jasim Mohammed<sup>3</sup>, Ahmed M. Amshawee<sup>4</sup>, Ali Zarrabi<sup>5,6\*</sup>

<sup>1</sup> Department of Biology, Faculty of Sciences, Shahid Bahonar University of Kerman, Kerman, Iran.

<sup>2</sup> Physiology Research Center, Kerman University of Medical Sciences, Kerman, Iran.

<sup>3</sup> Department of Microbiology, College of Medicine, Babylon University, Hilla City, Iraq.

<sup>4</sup> Department of Radiology, University of Hilla, Babylon, Iraq.

<sup>5</sup> Department of Biomedical Engineering, Faculty of Engineering and Natural Sciences, Istinye University, 34396, Istanbul, Türkiye

<sup>6</sup> Graduate School of Biotechnology and Bioengineering, Yuan Ze University, Taoyuan 320315, Taiwan

### \* Corresponding authors:

Sadegh Khorrami; Email: [s.khorrami.992@gmail.com](mailto:s.khorrami.992@gmail.com); ORCID: 0000-0002-1396-1316

Ali Zarrabi; Email: [ali.zarrabi@istinye.edu.tr](mailto:ali.zarrabi@istinye.edu.tr), ORCID: 0000-0003-0391-1769



## Abstract

Metal-based nanoparticles are emerging as a versatile platform to overcome critical challenges in the diagnosis and treatment of Alzheimer's disease (AD). This review provides a comprehensive synthesis of recent advances, structured around the three core domains of AD management: diagnostics, therapeutics, and theranostics. We discuss how the unique physicochemical properties of metals and metal oxides enable highly sensitive biosensing of amyloid and tau biomarkers, as well as high-contrast imaging modalities. The review then evaluates strategies for engineering metal-based nanoparticles to bypass the blood-brain barrier and achieve targeted accumulation, alongside their therapeutic roles in drug delivery, photothermal therapy, and modulating protein aggregation. Finally, we assess integrated theranostic systems that combine real-time imaging with targeted intervention. The key conclusion is that platforms based on metal-based nanoparticles, through their multifunctionality, offer a realistic pathway toward minimally invasive early diagnosis and targeted therapy. However, the field's future direction must prioritize rigorous standardization and advanced preclinical validation to translate these promising nanotechnologies from bench to bedside, ultimately advancing precision neurotheranostics for AD.

**Keywords:** Alzheimer's disease, Metal nanoparticles, Neurodegeneration, Theranostics



## 1. Introduction

Alzheimer's disease (AD) is a progressive neurodegenerative disorder that gradually erodes memory, identity, and independence, affecting over 55 million people worldwide and placing enormous emotional and socioeconomic burdens on patients and caregivers. Despite decades of research and the approval of cholinesterase inhibitors and NMDA receptor antagonists, current therapies at best slow symptom progression temporarily, leaving patients and caregivers yearning for more transformative solutions. Even the advent of monoclonal antibodies against amyloid- $\beta$  (A $\beta$ ), such as Aducanumab, lecanemab, and donanemab, has delivered only marginal clinical benefit and raised safety concerns,<sup>1</sup> underscoring the urgent need for innovative, dual-purpose strategies that can both diagnose and treat AD with precision and minimal toxicity and side effects.

Metal-based nanoparticles (MNPs) are tiny structures engineered at the 1-100 nm scale whose unique optical, magnetic, and electrical properties are rewriting the playbook for neurotheranostics (simultaneous therapy and diagnostics). Unlike their bulk counterparts, MNPs possess exceptional surface-area-to-volume ratios that enable high drug loading, controlled release, and facile functionalization with targeting ligands capable of traversing the blood-brain barrier (BBB).<sup>2</sup> Coupling therapeutic payloads with imaging modalities, ranging from magnetic resonance contrast to surface-enhanced Raman scattering (SERS), MNPs stand poised to illuminate early pathological changes in the AD brain while delivering neuroprotective or amyloid-clearing agents directly to affected regions.<sup>3,4</sup> Additionally, MNPs, such as gold (Au), cerium oxide (CeO<sub>2</sub>), iron oxide (Fe<sub>3</sub>O<sub>4</sub>), etc., exhibit intrinsic antioxidant activity and scavenging of reactive oxygen species (ROS), alongside anti-inflammatory actions that shift microglia toward a pro-resolving phenotype and reduce proinflammatory cytokines. In preclinical Alzheimer's models, these properties lower



oxidative neuronal damage, attenuate neuroinflammation, mitigate amyloid- and tau-related toxicity, and improve synaptic function and cognitive outcomes.<sup>3,5</sup>

This literature review aims to critically evaluate the current state of research on MNPs in AD, synthesizing evidence on three interconnected domains: diagnostic applications (sensitivity, specificity, and imaging modalities), therapeutic potential (drug delivery, neuroprotection, and amyloid/tau targeting), and combined theranostic platforms (design principles, *in vivo* performance, and translational challenges). The review will identify recurring strengths and limitations across studies, highlight gaps in preclinical and clinical evidence, and propose prioritized research directions to accelerate safe, effective translation of MNPs-based approaches for AD.

## 2. Methods

The databases searched for this study were PubMed, Web of Science, Scopus, and Google Scholar. Search terms consisted of combinations of “Alzheimer’s disease,” “metal nanoparticle,” “metal-based nanoparticle,” “gold nanoparticle,” “iron oxide,” “silver nanoparticle,” as well as specific metal NP types including cerium oxide, ruthenium, selenium, zinc oxide (ZnO), titanium dioxide, platinum, and Mn-Zn ferrite nanoparticles (these additional terms were identified from key references and preliminary scoping), together with “theranostic,” “diagnostic imaging,” and “drug delivery.” The search was limited to studies published in English from 2000 to the present, with an emphasis on the most recent decade.

Inclusion and exclusion criteria encompassed original research articles, systematic reviews, and meta-analyses reporting *in vitro*, *in vivo*, or clinical data directly on MNPs applied to AD diagnosis, therapy, or theranostics; this included studies describing MNP design, functionalization, imaging



performance, biodistribution, toxicity, or therapeutic efficacy. Exclusion criteria comprised the studies focusing solely on non-metal nanoparticles, purely theoretical/modeling papers without experimental validation, conference abstracts lacking full methods or data, and non-English publications.

Two independent reviewers screened titles and abstracts for relevance, followed by full-text review to determine eligibility. Discrepancies between reviewers were resolved through discussion or by involving a third reviewer. Results were synthesised narratively and organized by application domain (diagnostics, therapeutics, and theranostics) and NP class. Where sufficient homogeneous data were available, comparative tables summarising key performance metrics were created. Gaps and translational barriers were identified by cross-comparing efficacy, safety, reproducibility, and scale-up considerations across studies.

### 3. Pathophysiology of Alzheimer's disease

AD is a multifactorial disease with several intersecting pathogenic pathways. Among these, A $\beta$  pathology plays a central role. Abnormal cleavage of the amyloid precursor protein by  $\beta$ - and  $\gamma$ -secretases leads to accumulation of A $\beta$  peptides, which misfold into oligomers and insoluble fibrils. Soluble A $\beta$  oligomers are particularly neurotoxic, as they disrupt synapses and neuronal function. Over time, A $\beta$  aggregates form extracellular plaques in the brain, triggering local inflammation and oxidative injury. Tau pathology is the other hallmark. As a microtubule-associated protein, tau becomes abnormally hyperphosphorylated in AD and dissociates from microtubules. The hyperphosphorylated tau aggregates into paired helical filaments and intracellular neurofibrillary tangles (NFTs), which impair axonal transport and ultimately lead to neuronal death.<sup>6</sup> Notably, tau hyperphosphorylation and A $\beta$  pathology can potentiate each other;



for instance, tau pathology can exacerbate A $\beta$  aggregation and vice versa, creating a vicious cycle of neurodegeneration.<sup>7</sup>

Oxidative stress and mitochondrial dysfunction are also pervasive in AD and contribute to neuronal injury. A $\beta$  and tau accumulation, along with ageing-related changes, provoke an overproduction of reactive oxygen species (ROS) and reactive nitrogen species (RNS) that damage lipids, proteins, and DNA in the brain. Lipid peroxidation by ROS, for example, depletes membrane integrity and generates toxic aldehydes, while oxidatively damaged mitochondria fail to meet neuronal energy demands. This oxidative damage reduces antioxidant defenses and impairs synaptic plasticity, accelerating neurodegeneration.<sup>8–10</sup>

Neuroinflammation is another key aspect of AD pathogenesis. Aggregated A $\beta$  and tau deposits activate microglia and astrocytes, the immune cells of the central nervous system (CNS). Chronic activation of microglia leads to the release of proinflammatory cytokines (e.g. IL-1 $\beta$ , TNF- $\alpha$ ) and chemokines, as well as nitric oxide and ROS, which can injure surrounding neurons and synapses.<sup>11</sup> Acute inflammation, especially involving activated microglia, can aid A $\beta$  clearance. In AD, however, this inflammatory response becomes persistent and harmful, contributing to synaptic loss and neuronal death.<sup>12</sup>

Metal ion dysregulation, furthermore, is increasingly recognized as an important factor in AD (often termed the “metal hypothesis” of AD). Imbalances in brain metal homeostasis, particularly involving iron (Fe), copper (Cu), and zinc (Zn), have been linked to amyloid and tau pathology, oxidative stress, and cognitive decline.<sup>13</sup> Other factors, such as calcium dysregulation and glutamate excitotoxicity, genetic influences (e.g. APOE4 allele), and vascular changes, also interplay in AD progression.



In summary, AD involves a complex network of A $\beta$  accumulation, tau tangle formation, oxidative damage, and inflammation, all of which influence each other and lead to neuronal dysfunction and loss (**Fig. 1**). This complexity partly explains why therapies targeting only one aspect have had limited success. It also offers multiple targets for novel interventions, such as MNPs. The multifaceted pathological landscape of AD encourages exploring treatments that can address several processes simultaneously; for example, reducing A $\beta$ /tau burden, decreasing oxidative stress, and modulating metal ions and inflammation at the same time. The rationale for using MNPs in AD is that they provide a platform to target these interconnected pathways in an integrated or precise manner.

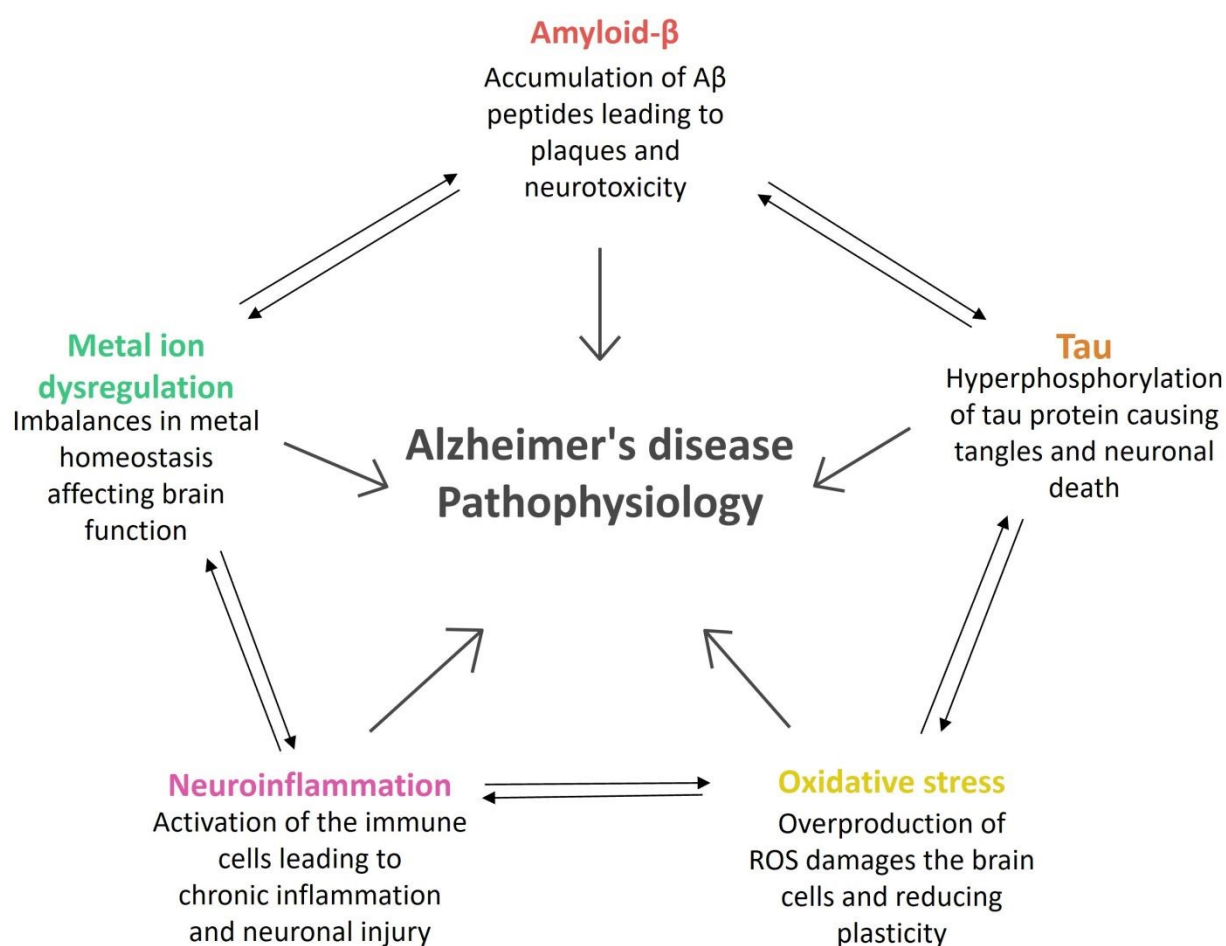


**Fig. 1** The figure summarizes the pathophysiology of AD, which involves a complex network of A $\beta$  accumulation, tau tangle formation, oxidative damage, and inflammation. These factors influence one another, ultimately leading to neuronal dysfunction and loss.

#### **4. Properties, functionalization, and biological interactions of MNPs**

##### **4.1. Physicochemical properties**

MNPs are tiny particles composed of metals like Au, silver (Ag), platinum (Pt), and others, typically ranging from 1 to 100 nm in size, and they possess unique physicochemical properties that distinguish them from other types of nanoparticles (NPs). Among these properties is localized surface plasmon resonance (LSPR). MNPs, especially those made of Au, Ag, and Pt, exhibit LSPR, a phenomenon that allows them to absorb and scatter light at specific wavelengths, making them highly effective in applications like biosensing, imaging, and photothermal therapy (PTT).<sup>14</sup> Their optical properties, such as the ability to produce vivid colors and strongly enhance Raman scattering—a phenomenon known as SERS—are utilized in various diagnostic and analytical techniques.<sup>15</sup> Certain MNPs, especially those made of Fe, exhibit magnetic properties like superparamagnetic behavior, which is exploited in magnetic resonance imaging (MRI), computed tomography (CT) scans, targeted drug delivery, and magnetic separation techniques.<sup>16</sup> MNPs also display exceptional catalytic activity due to their high surface area-to-volume ratio and the presence of active sites on their surfaces, making them highly efficient catalysts in chemical reactions, including those used in environmental remediation and industrial processes.<sup>17</sup> Additionally, MNPs exhibit excellent electrical conductivity, which is beneficial for the development of electronic devices, biosensors, and conductive inks.<sup>18</sup>

These unique properties make MNPs highly versatile and valuable in a wide range of applications, from medicine and environmental science to electronics and catalysis.<sup>19</sup> In the context of AD, these



traits enable MNPs to act as imaging contrast agents, carriers for drugs, or even catalysts for therapeutic reactions (such as antioxidant activity).<sup>20</sup> Their conductive properties enable highly sensitive electrochemical and impedance-based biosensors for early detection of AD biomarkers, like A $\beta$  and tau, and can improve signal transduction in nanoparticle-enhanced imaging probes. Another advantage is the ability to tune these properties. By adjusting synthesis methods, the nanoparticle's size, shape, and surface coatings can be controlled, thereby optimizing their behavior for crossing the BBB or targeting certain cells.

#### ***4.2. Surface functionalization and BBB crossing***

A major challenge in AD drug delivery is crossing the BBB, a tightly regulated interface that blocks most large or hydrophilic molecules from entering the brain. NPs can be engineered to overcome this barrier via surface functionalization (**Fig. 2**). By decorating NPs with specific ligands, researchers can exploit endogenous BBB transport mechanisms. For instance, coating NPs with transferrin, low-density lipoprotein, lactoferrin, melanotransferrin, insulin, folate, and N-acetylcholine (which bind to their receptors on brain endothelial cells) can trigger receptor-mediated transcytosis to ferry the NPs into the brain.<sup>21</sup> Various peptides have also been used for this purpose. The TGN peptide is a well-known BBB shuttle that, when attached to NPs, enhances their brain uptake. In one study, selenium NP (SeNP) functionalized with a dual peptide coating-TGN for BBB targeting and LPFFD peptide for binding A $\beta$ , successfully crossed the BBB and bound to amyloid plaques.<sup>22</sup> Cell-penetrating peptides (e.g. TAT from HIV) and apolipoprotein E (ApoE) fragments are additional strategies to increase NP brain entry. Surface modification with polyethylene glycol (PEG), known as PEGylation, is another common strategy to enhance biocompatibility and prolong circulation time. PEGylated NPs evade rapid clearance by the mononuclear phagocyte system.<sup>23</sup> Overall, a smart combination of size tuning and ligand



functionalization is used to optimize MNPs for brain targeting. Such functionalized MNPs act as “smart” nanocarriers that can seek out pathology in the brain.

## Nanoparticles Overcome Blood-Brain Barrier

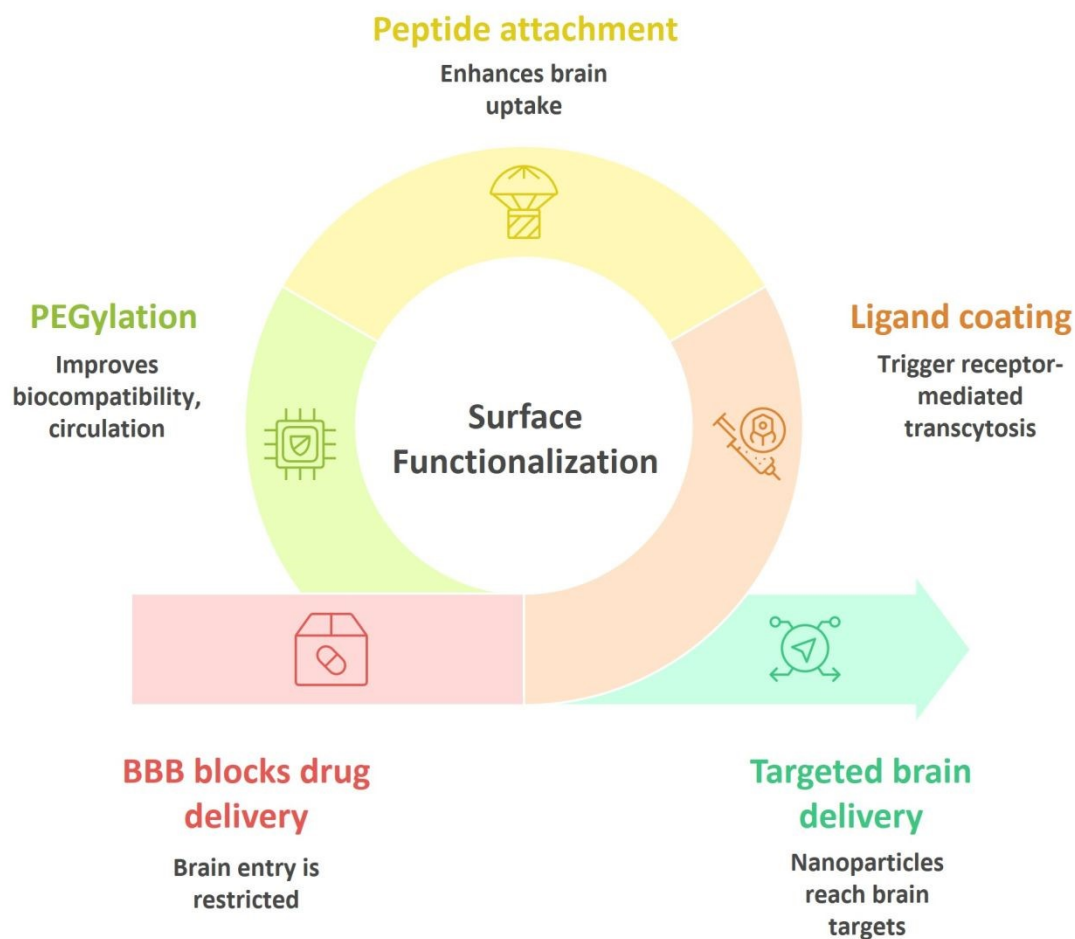


**Fig. 2** Surface functionalization strategies enabling NPs to overcome the BBB. Peptide attachment and ligand coating enable receptor-mediated transcytosis and enhanced brain uptake; PEGylation prolongs circulation and biocompatibility; and targeted delivery directs payloads to specific neural sites, while the intact BBB restricts unmodified drug entry.

### 4.3. Biological interactions



Once in the body, MNPs immediately interact with the biological environment, acquiring a “protein corona” of adsorbed biomolecules (proteins, lipids) that can change their identity as seen by cells. This corona can either mask or enhance targeting ligands and influence how NPs are recognized by the immune system.<sup>24</sup> MNPs with appropriate surface design can avoid excessive immune activation; however, if not, they might trigger complement activation or cytokine release.<sup>25</sup> Immune cells (microglia in the brain, macrophages in the periphery) might engulf NPs through phagocytosis or pinocytosis, which can be a desired outcome if the goal is to stimulate clearance of pathological peptides, or an undesired one if it removes the NPs before they act on neurons.<sup>26</sup>

Biocompatibility studies indicate that the route of administration and dose also matter. For example, intravascularly injected NPs circulate systemically and must be nonthrombogenic and non-immunogenic,<sup>27</sup> whereas intranasal delivery (explored for some AD nanomedicines) bypasses the blood route and directly accesses the brain along olfactory neurons, potentially allowing lower doses.<sup>28</sup> The fate of MNPs in the body depends on their composition. Some of these NPs biodegrade into ions, e.g. ZnO dissolves to Zn<sup>2+</sup>, which then is assimilated or excreted. Others, like Au, are inert and can persist unless cleared by phagocytes.<sup>3</sup> Encouragingly, certain MNPs can utilize biology to their advantage. For example, green synthesized NPs (using plant extracts to reduce metal ions) often come with a natural coating of biocompatible phytochemicals and have shown reduced toxicity and enhanced antioxidant effects in studies.<sup>29,30</sup>

## 5. Diagnostic applications of MNPs

Accurate and early diagnosis of AD is crucial for timely intervention. MNPs provide innovative tools for identifying and visualizing disease characteristics, thereby enhancing our understanding



of the molecular pathways that drive disease onset, progression, and treatment responses. By targeting key biomarkers such as A $\beta$  peptides, phosphorylated tau (p-tau), and neuroinflammation markers, NP probes can amplify weak signals and enable detection at lower concentrations than conventional assays. When integrated with established diagnostic modalities, including immunoassays, MRI, positron emission tomography (PET), and optical spectroscopy, metal NP platforms offer multimodal contrast, improved sensitivity, and the possibility of noninvasive or minimally invasive readouts. Engineered NP readouts range from plasmonic shifts and SERS to magnetic relaxation changes, colorimetric aggregation, and electrochemical signatures, creating flexible assay formats suitable for point-of-care screening, longitudinal monitoring, and research-grade molecular phenotyping.

### **5.1. Biomarkers and diagnostic modalities**

#### *A $\beta$ peptides, p-tau, neuroinflammation markers*

The pathophysiology of AD is anchored to two defining proteinopathies: the extracellular deposition of A $\beta$  plaques and the intracellular accumulation of hyperphosphorylated tau into NFTs. The predominant A $\beta$  isoforms of diagnostic interest are A $\beta$ <sub>1-40</sub> and A $\beta$ <sub>1-42</sub>; in particular, A $\beta$ <sub>1-42</sub> aggregates more readily and is more neurotoxic. In most biofluids, A $\beta$  levels decrease as brain deposits increase due to sequestration into plaques, creating characteristic signatures in cerebrospinal fluid (CSF) and, to a lesser degree, plasma.<sup>31,32</sup> In addition, tau protein, which normally stabilises microtubules, undergoes hyperphosphorylation at specific residues (T181, T231, S235, and S265), causing it to aggregate into NFTs and disrupt neuronal function. Both total tau and critical phosphorylated forms (p-tau) serve as reliable biomarkers for disease burden and progression. Several p-tau sites are under active investigation, including p-tau181, p-tau217, and p-tau231, which offer varying levels of early diagnostic power.<sup>31,33,34</sup>



The scope of biomarkers is ever-expanding. Neuroinflammation markers such as YKL-40 (chitinase-3-like protein 1, CHI3L1), glial fibrillary acidic protein (GFAP), triggering receptor expressed on myeloid cells 2 (TREM2), neurofilament light chain (NfL), and synaptic proteins, such as synaptosomal-associated protein 25 (SNAP-25), provide additional insight into neurodegeneration and complement the amyloid/tau focus.<sup>35</sup> Likewise, metal ions ( $\text{Fe}^{2+}$ ,  $\text{Cu}^{2+}$ ,  $\text{Zn}^{2+}$ ) have attracted attention as both contributors to pathogenesis (by promoting aggregation and ROS generation) and as diagnostic targets for imaging and biosensors, leveraging the unique affinity of A $\beta$  and tau for metal binding.<sup>36</sup>

## 5.2. Established diagnostic modalities

*CSF assays* are based on the quantification of A $\beta_{1-42}$ , total tau, and p-tau in CSF, which remains the current gold standard for AD diagnosis, with thresholds established for clinical use using assays like ELISA and mass spectrometry.<sup>37</sup> *PET imaging* is another method currently applied. The development of molecular imaging with PET and specific tracers, such as 11C-Pittsburgh Compound-B for amyloid and 18F-AV-1451 for tau, allows *in vivo* visualization of pathology, which correlates with cognitive decline and disease progression. Both amyloid and tau PET imaging can detect changes more than a decade before symptoms appear. New tracers for neuroinflammation (e.g., 11C-PK11195 for microglial activation) broaden these applications.<sup>38</sup> *MRI* is another widely used diagnostic method. Structural MRI detects atrophy in the medial temporal lobe and hippocampus, while advanced sequences and contrast agents identify microvascular and iron changes linked to amyloid plaques. While standard MRI lacks molecular specificity, contrast agents, particularly functionalised metal NPs, are being developed to target specific pathological features.<sup>39</sup>



Despite their diagnostic power, established methods face significant limitations. Of these, CSF collection requires lumbar puncture, which is invasive and often linked to adverse effects, deterring routine or repeated testing.<sup>40</sup> PET and high-field MRI rely on costly equipment and specialized staff; scans can run into thousands of dollars each, restricting widespread or population-based screening. Additionally, dilute and transient biomarkers, particularly early-stage oligomers of A $\beta$  and tau, frequently fall below the detection thresholds of conventional assays, undermining sensitivity.<sup>41</sup>

Most techniques remain confined to specialist clinics or research centers, precluding point-of-care access and delaying timely diagnosis.<sup>42</sup> In this regard, blood-based assays promise non-invasiveness, but they struggle with low analyte concentrations and interference from abundant plasma proteins, complicating reliable measurement of A $\beta$  and tau species.<sup>43</sup> Likewise, current modalities are generally insensitive to the soluble oligomeric forms that emerge in the prodromal phase, often a decade before symptoms appear, thus missing the critical window for early-stage intervention.<sup>44</sup> These deficiencies underscore the urgent need for minimally invasive, highly sensitive, and cost-effective biosensing and imaging technologies suited to routine use in primary or community settings.

### ***5.3. MNPs-based diagnostic platforms and readouts***

MNPs have become central to the development of innovative diagnostic platforms for AD, owing to their unique physicochemical properties, high surface reactivity, and strong interaction with biological targets. Their versatility enables integration into diverse readout systems, ranging from biosensors and colorimetric assays to advanced spectroscopic and electrochemical techniques, thereby enhancing sensitivity and specificity in biomarker detection. In addition, nanoparticle-



based strategies extend beyond *in vitro* assays to *in vivo* imaging modalities, including MRI, micro-computed tomography ( $\mu$ CT), and fluorescence/photoacoustic imaging, providing powerful tools for early diagnosis and comprehensive monitoring of AD progression.

As summarized in Table 1, a comparison of recent diagnostic platforms reveals distinct trade-offs between sensitivity and translational readiness. SERS and electrochemical (EC) immunosensors consistently achieve the highest sensitivity, with limits of detection (LODs) reaching the femtomolar range, making them suitable for detecting trace biomarkers in early-stage pathology. In contrast, colorimetric assays and molecularly imprinted polymer (MIP) test strips, while less sensitive, offer rapid, visual readouts that are more adaptable for point-of-care applications. Notably, an increasing number of platforms are being validated in complex human matrices, such as serum and fingerprick blood, moving beyond buffer solutions and artificial cerebrospinal fluid.

### 5.3.1. Biosensors

#### *Colorimetric assays*

MNPs-based colorimetric assays exploit the unique optical properties of particles such as Au, Ag, and their alloys. Gold nanoparticles (AuNPs), in particular, exhibit LSPR with visible color changes upon aggregation/dispersion or biomolecular interaction, enabling simple, rapid, and instrument-free detection modalities. Zhu et al. (2018) developed an aptamer-functionalized AuNPs colorimetric sensor for  $A\beta_{1-40}$  oligomers, demonstrating a detection limit of 0.56 nM and high recovery in artificial CSF.<sup>45</sup> Similarly, Zhou et al. (2015) used aggregation of AuNPs for  $A\beta_{1-40}$  colorimetric sensing in the presence of copper ions with a detection limit of 0.6 nM, validated in human serum.<sup>46</sup> Regarding point-of-care test strips, Moreira et al. (2021) reported a MIP cellulose test strip for  $A\beta_{42}$  that enabled naked-eye quantification with a detection limit of 0.71



ng/mL, showing robustness for real-world sample matrices and cost-effectiveness suited to decentralized diagnostics.<sup>47</sup>

Colorimetric detection of tau, though less reported, has been achieved via AuNP-antibody conjugates. In this regard, Neely et al. (2009) detected tau to 1 pg/mL, two orders of magnitude below CSF concentrations in AD, demonstrating potential for early-stage disease screening.<sup>48</sup> Notably, colorimetric assays are straightforward, offering readout by eye or smartphone and rapid turnaround for point-of-care screening. However, they are prone to sample matrix effects, variable accuracy in complex fluids and require surface functionalization to minimize non-specific aggregation.<sup>49</sup>

#### *SERS-based assays*

SERS is enabled by the signal amplification that occurs when molecules are adsorbed on, or in proximity to, metallic nanostructures (such as Au/Ag NPs, nanorods, or nanostars). In AD diagnostics, a label-free SERS biosensor with AuNPs on indium tin oxide was fabricated for A $\beta$ <sub>1-40</sub>, providing a detection window of 100 fg/mL–1  $\mu$ g/mL.<sup>50</sup> Also, SERS nanoprobe synthesized with Ag NP shells functionalized with A $\beta$  antibody have been employed for multiplexed detection of A $\beta$ <sub>1-40</sub> and A $\beta$ <sub>1-42</sub> in blood, achieving LODs of 0.25 and 0.33 pg/mL, respectively.<sup>51</sup> Another SERS sandwich immunoassay has been developed for tau protein with a detection limit as low as 25 fM. Also, an Au nanowire SERS array was integrated for dual detection of A $\beta$  and tau at fg/mL levels.<sup>33,52</sup> In a study, Garnaik et al. (2024) showed that SERS nanoprobe functionalized with dyes (Rhodamine B and Coumarin 6) and metallic particles selectively adsorbed A $\beta$ <sub>42</sub> and tau protein, with spectral features correlating to peptide secondary structure and binding affinity.<sup>53</sup>

Despite these advances, several technical challenges hinder widespread clinical adoption. Chief among them is the reproducibility of hot spots, localized regions of intense electromagnetic



enhancement, which are critical for consistent signal amplification. Variability in nanostructure fabrication and sample placement can lead to significant fluctuations in signal intensity. Additionally, SERS signal normalization remains difficult due to environmental and matrix effects, complicating reliable biomarker quantification. To address this, researchers have begun embedding internal standard NPs into assay designs to stabilize signal output.<sup>54</sup> Finally, translating SERS technology into user-friendly formats for non-expert operators requires robust assay integration, intuitive interfaces, and scalable manufacturing, areas that are still under active development.<sup>50</sup>

#### *Electrochemical immunosensors*

Electrochemical sensors convert biomolecular binding into an electrical signal, and benefit markedly from surface modification with metal NPs (Au, Ag, Fe<sub>3</sub>O<sub>4</sub>, and composites) to enhance electron transfer, immobilize recognition elements, and amplify signals.<sup>55</sup> In a study, Negahdary and Heli (2019) created an electrochemical peptide-based biosensor using an Au nanostructured electrode and A $\beta$ <sub>1-42</sub>-binding peptide, achieving a LOD of 0.2 pg/mL and fair stability in mock CSF and serum.<sup>56</sup> For tau/p-tau detection, Kong et al. (2024) presented an Au nanoparticle-enhanced aptamer sensor for p-tau<sub>231</sub> with a broad linear range (10–10<sup>7</sup> pg/mL) and an LOD of 2.31 pg/mL, adequate for plasma-based screening.<sup>57</sup> Similarly, Razzino et al. (2020) detected tau to 1.7 pg/mL in plasma and brain tissue using an Au/PAMAM dendrimer electrode.<sup>58</sup> Also, a biosensor based on platinum-zeolitic imidazolate frameworks (Pt@ZIF-8) nanocomposite electrode was recently designed that specifically targets cis-p-tau, with femtogram-range LOD and strong selectivity over trans-tau and total tau, crucial for early pathological confirmation.<sup>59</sup> In addition, researchers recently developed a multi-analyte device detecting t-tau, p-tau<sub>181</sub>, A $\beta$ <sub>40</sub>,



and A $\beta$ 42 on an Au@graphene nanocomposite, reaching sub-picogram detection with recoveries >90% in plasma.<sup>60</sup>

Emerging trends and challenges in next-generation biosensing technologies demonstrate both the promise and limitations of advanced platforms. Aptamer-based (nucleic acid) sensors offer enhanced specificity and reusability, metal-organic frameworks (MOF)-based sensors provide robust supports and catalytic activity, and integration with microfluidics streamlines on-chip assays for rapid, portable diagnostics.<sup>34,57</sup> It is worth noting that these systems offer outstanding detection limits, suitability for multiplexing, and miniaturisation for point-of-care applications. However, they face the risk of signal drift with long-term use, sensitivity to surface fouling, and the cost of fabrication and validation in clinical matrices.<sup>61</sup>

### 5.3.2. Nanoparticle-enhanced brain imaging

#### *MRI agents*

MRI is a non-invasive diagnostic technique that generates high-resolution images by detecting the relaxation behavior of hydrogen nuclei in tissues exposed to a strong magnetic field and radiofrequency pulses. Image contrast depends on differences in relaxation times ( $T_1$  and  $T_2$ ), which can be selectively altered by contrast agents to improve the visibility of specific structures or pathologies.<sup>62</sup> MNPs, especially  $Fe_3O_4$  and gadolinium (Gd), serve as advanced MRI contrast agents, offering higher relaxivity, targeted functionalization, and in some cases, dual diagnostic-therapeutic (“theranostic”) potential.<sup>63</sup>

Iron oxide NPs have been extensively explored for  $T_2$  and  $T_1$ -weighted imaging. PEGylated, antibody or peptide-functionalized iron oxide NPs (IONPs) have demonstrated successful targeting of A $\beta$  plaques and tau aggregates in transgenic mouse models.<sup>64</sup> In particular,



superparamagnetic iron oxide NPs (SPIONPs) are excellent T2 MRI contrast agents. Also, Mn-Zn ferrite (MZF) NPs were conjugated with Pittsburgh compound B (PiB, an amyloid-specific ligand) and coated with a biocompatible polymer; the resulting ~100 nm “PiB-MZF” NPs showed high relaxivity and specifically bound to A $\beta$  plaques in AD mouse brain sections.<sup>65</sup> Additionally, Gd-based NPs have shown promising performance in this regard. Plissonneau et al. (2016) functionalized Gd-based MRI NPs with A $\beta$ -targeting peptides (KLVFF, LPFFD), showing enhanced MRI positive contrast and plaque-specific labeling, with r1/r2 relaxivity outperforming clinical Gd agents.<sup>66</sup>

Another approach is to apply multimodal NPs; for example, NPs that are both fluorescent and magnetic, allowing optical tracking and MRI. Nanoplatfoms, such as Fe-MIL-88B-NH<sub>2</sub>, Ru@MIL-101(Al), have been developed that incorporate MRI, fluorescence, or PET capabilities. These agents facilitate simultaneous imaging and biomarker quantification.<sup>31,63</sup> Quantum dots (QDs; semiconductor nanocrystals) are also fluorescent and have been used experimentally to label amyloid deposits. However, many QDs contain toxic metals, such as cadmium (Cd), raising toxicity concerns.<sup>67</sup>

#### *CT/ $\mu$ CT contrast*

CT and  $\mu$ CT scans are imaging techniques that use rotating X-ray beams and computer reconstruction to generate detailed cross-sectional images of internal structures. The contrast in CT images arises from differences in X-ray attenuation, which depends largely on the density and atomic number of the material being scanned. Materials with higher atomic numbers attenuate X-rays more strongly, producing brighter signals and sharper contrast in the resulting images.<sup>68</sup> Among the various nanoparticulate materials, Au, Fe<sub>3</sub>O<sub>4</sub>,  $\gamma$ -Fe<sub>2</sub>O<sub>3</sub>, Gd, and related heavy metals



have gained particular attention due to their high X-ray attenuation, tunable surface chemistry, and biocompatibility.

AuNPs have a high atomic number ( $Z = 79$ ), which gives them superior X-ray attenuation compared to traditional iodine-based contrast agents. This property allows for improved imaging resolution. Additionally, AuNPs can carry a high payload of contrast-generating material, exhibit strong X-ray attenuation, possess excellent biocompatibility, and offer customizable surface chemistry. They also come in various sizes and shapes, making them versatile for different applications.<sup>69</sup> Regarding AD, Betzer et al. (2017) demonstrated that insulin-coated AuNPs successfully crossed the BBB *in vivo* in Balb/C mice, as observed via CT imaging two hours post-injection. These NPs localized to brain regions associated with neurodegeneration,<sup>70</sup> supporting their potential for CT-based brain imaging in AD models. The primary mechanism of these particles for brain entry was receptor- and adsorptive-mediated transcytosis, confirmed both *in vivo* and in an *in vitro* BBB setup.<sup>71</sup>

#### *Fluorescence/Photoacoustic imaging*

Fluorescence imaging relies on the excitation of fluorophores by light, which then emit photons at longer wavelengths to visualize cellular and tissue structures with high sensitivity. Photoacoustic imaging, in contrast, converts absorbed optical energy into ultrasonic waves, combining the molecular specificity of light with the deeper penetration of ultrasound. Together, these optical techniques enable non-invasive, high-resolution imaging of biological processes, especially when enhanced by nanoparticle-based contrast agents.<sup>72</sup> AuNPs functionalized with CRANAD-2 have demonstrated a marked enhancement in fluorescence intensity. CRANAD-2 is a curcumin-derived near-infrared (NIR) probe that exhibits high affinity for  $A\beta_{40}$  aggregates. The resulting nanoconjugate enables ultrasensitive detection of  $A\beta$  both *ex vivo* and *in vivo*, offering a promising



platform for early-stage AD.<sup>33,73</sup> Also, recently developed second near-infrared window (NIR-II, 1000-1750 nm) fluorescent AuNPs and single-walled carbon nanotubes provided deeper tissue penetration and higher S/N ratios for *in vivo* imaging.<sup>74</sup> Jang et al. (2022) fabricated a MOF-derived carbon NP for NIR-responsive photoacoustic dissociation and detection of A $\beta$  aggregates, opening avenues for non-invasive, real-time imaging and even therapeutic modulation of plaques.<sup>75</sup> Likewise, QDs and metal oxide nanomaterials, such as lead sulfide (PbS) QDs and Erbium (Er)-based NPs, and rare-earth doped NPs, combine tunable emission, high photostability, and biocompatibility for label-free tau and A $\beta$  imaging at femtomolar sensitivity.<sup>74,76,77</sup>



**Table 1.** Major metal-based platforms for AD diagnosis.

Platform type	Metal/Nanomaterial	Target Biomarker(s)	Sensitivity (LOD)	Readout	Matrix / Validation	Ref.
<b>Colorimetric assay</b>	AuNPs	A $\beta$ 1–40 oligomer	0.56 nM	Visible absorbance	aCSF, serum	45
<b>MIP test strip</b>	AuNPs/cellulose	A $\beta$ -42 peptide	0.71 ng/mL	Visual/RGB	Serum/real samples	47
<b>SERS</b>	AuNP/AgNP/Au nanorods	A $\beta$ /tau proteins	0.25 pg/mL (A $\beta$ ), 25 fM (tau)	Raman	Blood, CSF	50,52
<b>EC immunosensor</b>	AuNPs, Pt@ZIF-8	A $\beta$ , p-tau, t-tau, cis-tau	0.2 pg/mL – 1 fg/mL	Electrochemical	CSF, plasma, brain tissue	57,59
<b>MRI agent</b>	Fe <sub>3</sub> O <sub>4</sub> , Gd-NPs, IONP	A $\beta$ plaques, tau aggregates	Preclinical visualization	MRI	Animal, human brain sections	66,78
<b>CT/<math>\mu</math>CT contrast</b>	AuNPs, IONP	Amyloid plaques	$\mu$ CT contrast	CT/ $\mu$ CT	Murine models, in vivo brain	52,71
<b>Fluorescence /photoacoustic</b>	Au nanorods, QDs, ErNPs	A $\beta$ aggregates, tau, NfL	0.001 nM – deep tissue	NIR/NIR-II, PA	Ex vivo, in vitro, animal	73,74



**Multiplexed PoC**

AuNPs/AgNPs

A $\beta$ , tau, NfL

fg/mL, ultralow

Multiplexed chip

Serum, fingerprick blood

33,79,80

**SERS/EC chip**

## Abbreviations:

LOD: limit of detection, AuNPs: gold NPs, aCSF: artificial cerebrospinal fluid, MIP: molecularly imprinted polymer, ng: nanogram, RGB: red green blue, SERS: surface-enhanced Raman scattering, pg: picogram, fM: femtomolar, EC: electrochemical, p-tau: phosphorylated tau, MRI: magnetic resonance imaging, Fe<sub>3</sub>O<sub>4</sub>: magnetite (iron(II, III) oxide), Gd-NPs: gadolinium NPs, IONP: iron oxide nanoparticle, CT/ $\mu$ CT: computed tomography/micro-computed tomography, QDs: quantum dots, ErNPs: erbium-doped NPs, NfL: neurofilament light chain, NIR: near-infrared, PA: photoacoustic, Pt@ZIF: platinum NPs within a zeolitic imidazolate framework.

## 6. Therapeutic applications of MNPs

MNPs offer a multifunctional therapeutic toolbox for AD by combining targeted delivery, intrinsic bioactivity, and modular surface chemistry. As nanocarriers, they improve BBB transport and drug bioavailability, enable sustained or targeted release, and can be functionalized for receptor-mediated uptake; several platforms also serve as vectors for gene delivery and other advanced payloads. Many metal-based particles exhibit intrinsic antioxidant and anti-inflammatory properties or can be loaded with neuroprotective agents to scavenge reactive oxygen species, suppress microglial activation, and preserve neuronal function. Additionally, engineered NPs can bind, disaggregate, or promote enzymatic/phagocytic clearance of toxic protein aggregates (A $\beta$  and tau) (**Fig. 3**). When combined with imaging or responsive elements, they enable theranostic monitoring of treatment response.



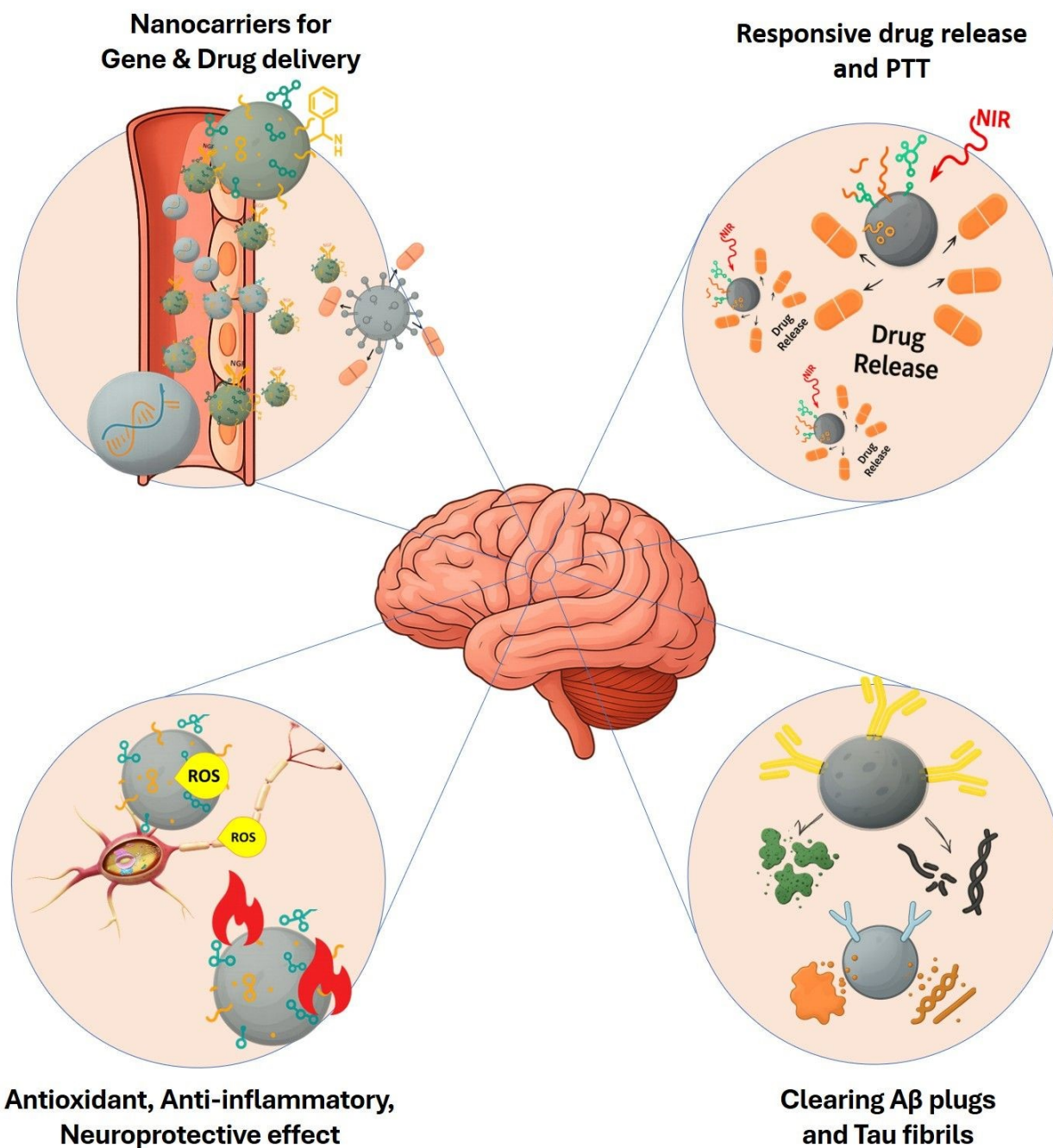


**Fig. 3** Therapeutic applications of metal NPs in brain-related therapies. Nanocarriers for drug and gene delivery: MNPs ferry conventional drugs, genes and neurotrophic factors across the BBB, enhancing bioavailability and targeting (e.g., curcumin-CeO<sub>2</sub> NPs; resveratrol-SeNPs-TGN; quercetin-SPIONPs-NGF). Additionally, PEGylated Au and Fe<sub>3</sub>O<sub>4</sub> NPs deliver siRNAs targeting APOE4, BACE1, or SOX9, functioning as robust non-viral vectors and supporting the control of neural stem cell differentiation. Responsive drug release and photothermal therapy (PTT): Ruthenium nanoparticles (RuNPs) and



polydopamine-Ru nanosystems enable near-infrared (NIR)-triggered drug release, reactive oxygen species (ROS) scavenging and heat-mediated cytotoxicity. Antioxidant, anti-inflammatory and neuroprotective effects: Au, Ag, CeO<sub>2</sub>, Se, ZnO and Ru/RuO<sub>2</sub> NPs scavenge free radicals, bolster endogenous antioxidant defenses, reduce A $\beta$  aggregation and attenuate neuroinflammation. Clearance of protein aggregates: SPIONPs and AuNPs conjugated to anti-A $\beta$  or tau antibodies promote microglial uptake, inhibit fibril formation and degrade pathological plaques.

### 6.1. Nanocarriers for drug delivery

MNPs can ferry conventional drugs, genes, or neurotrophic factors into the brain, improving their bioavailability and targeting. MNPs improve drug delivery by protecting therapeutic molecules from degradation, enhancing uptake by neurons, and concentrating them in the brain (thus requiring lower systemic doses). Given the BBB's restrictive nature, NPs act as Trojan horses to smuggle drugs in. NPs have been used to carry antioxidants and neuroprotective compounds that would not easily reach the brain on their own.<sup>81,82</sup> For example, several natural compounds, such as curcumin and resveratrol, have poor brain bioavailability but exhibit anti-AD activity. Loading these compounds into NPs, like curcumin-loaded CeO<sub>2</sub> NPs or resveratrol-loaded SeNPs, significantly enhances their efficacy in AD models.

A specific example is SeNPs (8 nm) that were loaded with resveratrol, as a neuroprotective agent, and decorated with a BBB-translocating peptide TGN (14 nm). Oral administration of these nanocomposites reduced neuronal integrity impairment and morphological changes in the hippocampus, increased hippocampal A $\beta$  clearance, and effectively inhibited A $\beta$  deposition in the hippocampus. Furthermore, these nanocomposites modulated the neurotransmitters affecting the AD pathogenesis, including  $\gamma$ -aminobutyric acid (GABA), glutamate (Glu), acetylcholine (ACh), norepinephrine (NE), histidine (His), tyrosine (Tyr) and tryptophan (Trp) (**Fig. 4**). These NPs even modulated gut microbiota favorably in AD mice.<sup>83,84</sup> Another study conjugated nerve growth factor (NGF, a large protein) and the polyphenol quercetin onto SPIONPs. This nanocomplex



successfully promoted neuronal differentiation and branching in PC12 cells, indicating that the NPs delivered their payloads in bioactive form, which highlights its therapeutic potential for AD.<sup>85</sup> In animal models of AD, SPIONPs conjugated with A $\beta$  oligomer antibody and a class A scavenger receptor activator effectively inhibit A $\beta$  oligomer-induced toxicity and promote microglial removal of A $\beta$ . These interventions notably enhance cognitive performance and reduce AD-related brain pathology.<sup>86</sup> Such results illustrate how nanocarriers can broaden the repertoire of AD therapeutics by enabling compounds that otherwise couldn't effectively treat the brain.



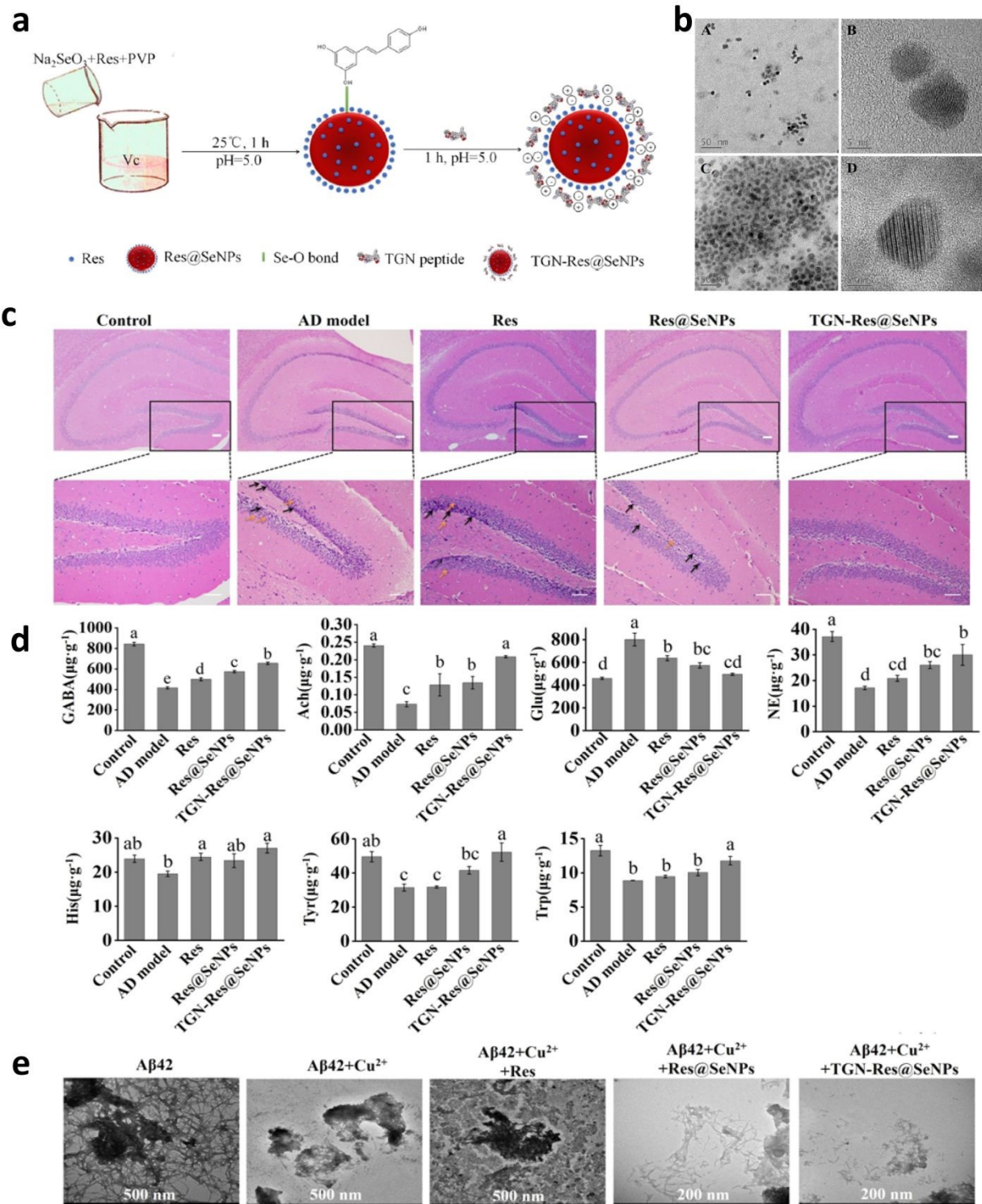


**Fig. 4** Resveratrol loaded on selenium NPs functionalized with BBB-translocating peptide TGN (TGN-Res@SeNPs). a) Schematic illustration for the synthesis of TGN-Res@SeNPs. b) High-resolution transmission electron microscopy (TEM) of NPs: Res@SeNPs (bA, bB) and TGN-Res@SeNPs (bC, bD).



c) Representative images of H&E staining showing the effects of TGN-Res@SeNPs treatment on histopathological changes and amyloid deposition in the brain of AD model mice. d) Concentration of  $\gamma$ -aminobutyric acid (GABA), glutamate (Glu), acetylcholine (ACh), norepinephrine (NE), histidine (His), tyrosine (Tyr) and tryptophan (Trp) in the hippocampus. e) Morphology of the  $\text{Cu}^{2+}$ ,  $\text{A}\beta_{42}$  monomer incubated with or without Res, Res@SeNPs, or TGN-Res@SeNPs for 3 days. Reproduced with permission from <sup>83</sup>.

At a higher level, NPs can be specifically engineered for responsive drug release, allowing for targeted delivery of medication directly to the disease site. For example, researchers have developed NGF functionalised ruthenium NPs (RuNPs), which exhibit an excellent photothermal effect. Under NIR irradiation, this nanocomposite can effectively penetrate the BBB and respond to phase changes in the affected area, leading to the release of NGF. This release helps inhibit tau hyperphosphorylation, reduces oxidative stress, and, importantly, restores nerve damage while maintaining neuronal structure. As a result, this approach significantly improves learning and memory in mice with AD (**Fig. 5**).<sup>87</sup> A team of researchers has unveiled a polydopamine-Ru nanosystem (PDA-Ru) that functions simultaneously as a NIR PTT agent, ROS scavenger, and hydrogen peroxide ( $\text{H}_2\text{O}_2$ ) catalyst. *In vivo* experiments indicate that PDA-Ru combined with NIR light effectively reduces  $\text{A}\beta$  accumulation, thereby restoring the regulatory functions of microglia. Ultimately, this approach alleviates memory impairments in the AD mouse model.<sup>88</sup>



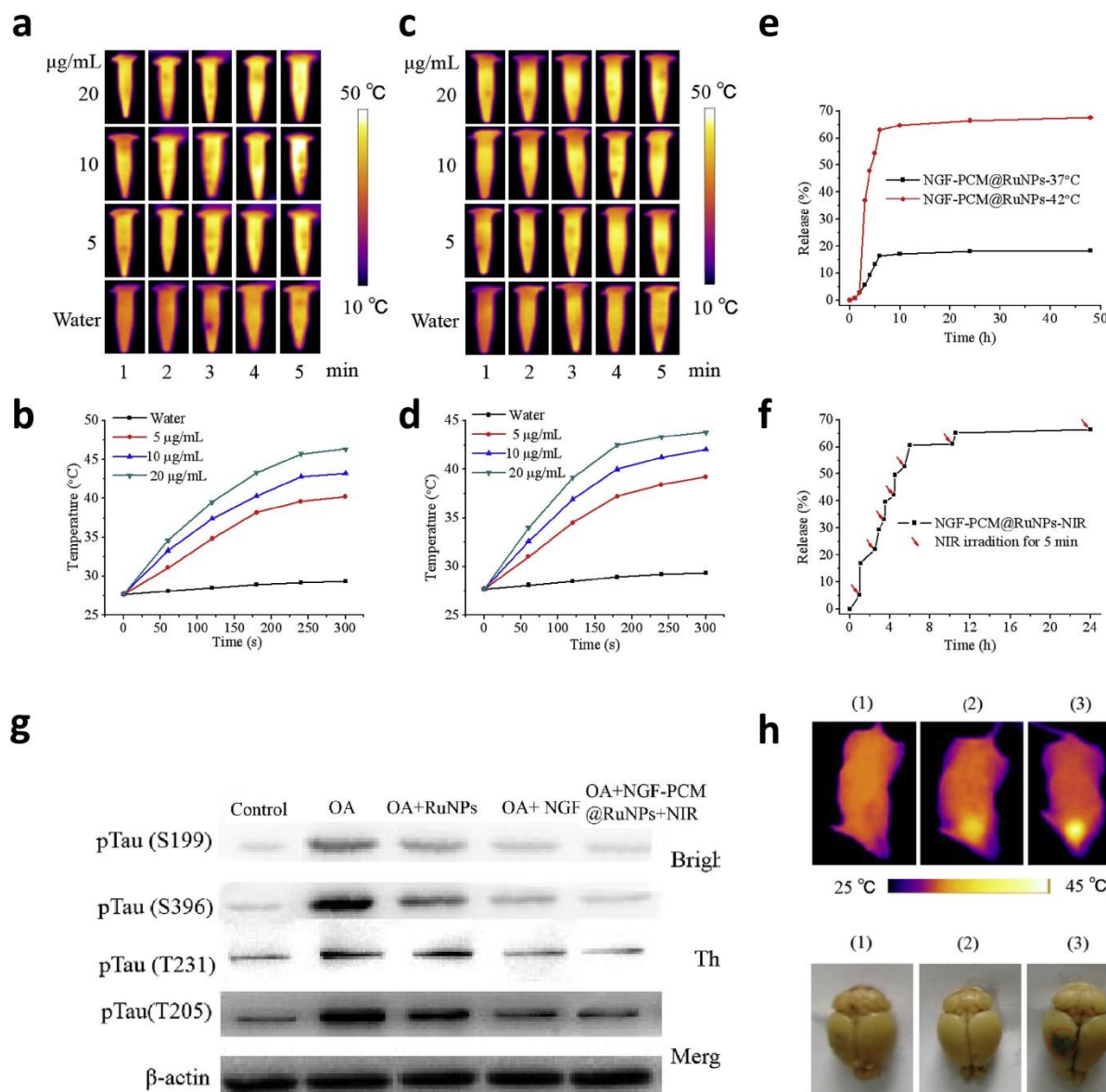


**Fig. 5** Photothermal heating and temperature-triggered release of RuNPs and NGF-PCM@RuNPs. Thermal images and time-temperature traces under 808 nm NIR irradiation show a clear photothermal effect for Ru NPs compared with water controls. **a** and **b** respectively show thermal images and temperature-time curves for water and Ru NPs; water shows insignificant heating while RuNPs yield a concentration-dependent temperature increase. Also, **c** and **d** show thermal images and temperature-time curves, respectively, for NGF-PCM@RuNPs under identical irradiation conditions, demonstrating a similarly strong, concentration-dependent photothermal response. **e** shows cumulative release profiles of NGF-PCMs@RuNPs at 37  $^{\circ}\text{C}$  and 42  $^{\circ}\text{C}$ , indicating accelerated release at 42  $^{\circ}\text{C}$ . **f** demonstrates cumulative release with and without a 5



min NIR pulse, indicating markedly enhanced release following NIR irradiation. **g**) Western blot analysis of hyperphosphorylated tau (p-tau) at serine 199, 396, and threonine 231, 205 epitopes in SH-SY5Y cells shows that NGF-PCM@RuNPs combined with NIR significantly reduced tau hyperphosphorylation (OA: Okadaic acid, which induces hyperphosphorylation). **h**) Thermal images (top row) show 808 nm NIR heating to ~42 °C only in the NGF-PCM@RuNPs + NIR group, and corresponding brain photographs (bottom row) show Evans blue staining only in the NGF-PCM@RuNPs + NIR group, indicating localized, temperature-dependent BBB disruption and enhanced NP penetration. (1): NGF-PCM@RuNPs; (2): NIR, (3): NGF-PCM@RuNPs + NIR, PCM: phase change material. Reproduced with permission from <sup>87</sup>.

The ability to combine multiple agents is another advantage. A single NP can be multifunctional. There are demonstrations of “combo” nanodrugs, such as IONPs with one surface ligand targeting amyloid and another surface carrying an enzyme or siRNA to degrade A $\beta$ .<sup>89</sup> This will be discussed in depth in the “theranostic potential of metal NPs” section.

## 6.2. Antioxidant, anti-neuroinflammation, and neuroprotective effects

Many MNPs naturally counteract some AD pathological processes, such as oxidative stress or neuroinflammation. The antioxidant properties are notable in several MNPs. For example, AuNPs have been reported to reduce oxidative stress and inflammation in neural cells. They can scavenge free radicals and also modulate signalling pathways. AuNPs were shown to suppress activation of NF- $\kappa$ B (a proinflammatory transcription factor) and downregulate caspase enzymes, thereby reducing apoptosis in neuron cultures.<sup>90</sup>

AgNPs likewise possess potent antioxidant capabilities. These NPs can directly neutralise ROS without needing enzymatic cofactors. They help maintain mitochondrial function, ensuring ATP production, and prevent excessive H<sub>2</sub>O<sub>2</sub> formation in cells.<sup>30</sup> In AD models, treatment with bio/green synthesized AgNPs prevented cognitive deficits, which correlated with increased levels



of glutathione (GSH, an endogenous antioxidant) and lower lipid peroxidation markers. AgNPs also inhibited acetylcholinesterase (AChE) in these models, which can increase acetylcholine levels and improve cognition.<sup>91</sup>

CeO<sub>2</sub> NPs, also known as ceria or cerium dioxide NPs, are often described as regenerative antioxidants: they can mimic the activity of catalase and superoxide dismutase (SOD) enzymes. In neuronal studies, CeO<sub>2</sub> NPs protected against A $\beta$ -induced mitochondrial fragmentation and cell death.<sup>92</sup> Moreover, a cleverly designed core-shell CeNP@MnMoS<sub>4</sub> NP was able to reduce A $\beta$  aggregation (especially Cu-induced aggregation) and concurrently lower ROS, demonstrating how nanoceria could address metal-linked oxidative toxicity.<sup>93</sup>

Likewise, SeNPs provide selenium in a nano-form that boosts antioxidant defenses (Se is a cofactor for glutathione peroxidases and thioredoxin reductase). SeNPs have been shown to upregulate antioxidant enzymes and reduce oxidative stress in the brain.<sup>94</sup> Notably, these NPs can also directly influence protein aggregation. One report found that SeNPs biodegraded existing amyloid fibrils into non-toxic aggregates and lessened tau hyperphosphorylation and neuroinflammation, ultimately slowing AD progression in a mouse model. This multi-modal neuroprotective action (antioxidant + anti-amyloid + anti-tau) is highly desirable.<sup>95</sup>

ZnO NPs (ZnO NPs), interestingly, can act as a zinc delivery system. Moderate zinc supplementation via ZnO NPs in zinc-deficient AD models helped normalize zinc levels, which in turn enhanced the activity of zinc-dependent A $\beta$ -degrading enzymes and receptors.<sup>96</sup> In a study, ZnO NPs crossed the BBB and significantly reduced amyloid plaque burden, lowered neuroinflammatory cytokines (IL-6, IL-18), and improved spatial memory in an AD mouse model.<sup>97</sup> These NPs also inhibited AChE, providing pro-cholinergic effects.<sup>98</sup>



RuNPs also showed antioxidant activity, mainly through suppressing  $Zn^{2+}$ -A $\beta$ -mediated generation of ROS. They can also inhibit intracellular A $\beta$ 40 fibrillation and its corresponding neurotoxicity in PC12 cells.<sup>99</sup> Similar functions have also been reported for RuO<sub>2</sub>. These NPs enter cells by endocytosis and restore the oxidative stress balance of cells.<sup>100</sup>

### 6.3. Clearing protein aggregates and enhancing clearance

Another strategy is to use MNPs to help remove toxic A $\beta$  or tau from the brain. One approach is immunotherapy via NPs. IONPs or AuNPs can be conjugated with antibodies or peptides that target A $\beta$ , serving as nanoscopic “garbage collectors.” For instance, SPIONPs coated with an antibody fragment against A $\beta$  oligomers were shown to bind A $\beta$  species and promote their phagocytosis by microglia.<sup>86</sup> In an AD mouse model, these antibody-conjugated SPIONPs increased microglial uptake of amyloid and reduced the overall A $\beta$  burden, leading to improved cognitive performance. The magnetic properties of these NPs enable external magnetic fields to guide them, potentially pulling bound amyloid out of the brain, an experimental technique that some researchers have explored *in vitro*.<sup>4</sup> Another study similarly used magnetic nanoclusters with an A $\beta$ -binding peptide; when applied to AD-model mice, they not only trapped A $\beta$  but also, under a magnetic field, helped disrupt plaque structure and facilitate clearance.<sup>101</sup> In the case of tau, tau-targeted NPs, for example, polymer NPs with anti-tau antibodies or tau aggregation inhibitor molecules on their surface, are being investigated to intercept tau seeds and prevent the spread of tau pathology.<sup>102</sup>

One exciting development in this field is the use of PTT to destroy protein aggregates. AuNPs can convert absorbed NIR light into heat efficiently. Researchers attached A $\beta$ -recognizing peptides to AuNPs, allowed them to bind to amyloid aggregates, and then applied a laser at the particles' resonance frequency. The localized photothermal effect selectively ablated the amyloid aggregates



*in vitro* without damaging surrounding tissue. Because the AuNPs only heat up where the laser is focused (for instance, at a suspected plaque site), this method could potentially disaggregate plaques in a controlled manner.<sup>103,104</sup> Photothermal disruption of A $\beta$  fibrils has been demonstrated in cell culture and is being refined for safety/biocompatibility and precision in tissues.<sup>105</sup> RuNPs also have strong photothermal responses to NIR light and have been shown to cross the BBB under NIR irradiation. RuNPs in an AD mouse model inhibited tau aggregation, and when combined with light exposure, they offered the additional benefit of triggered drug release and mild hyperthermia to enhance clearance.<sup>87</sup> Likewise, RuO<sub>2</sub> helps reduce A $\beta$  toxicity by eliminating accumulated ROS *in vivo*.<sup>100</sup>

#### 6.4. Gene therapy and other novel approaches

While human trials have not yet commenced, metal NPs are emerging as versatile nonviral vectors for gene therapy in AD. Their ability to protect nucleic acid cargo, cross biological barriers, and enable targeted delivery positions them as promising alternatives to viral vectors, which face safety concerns and limited packaging capacity. Recent preclinical studies have substantially expanded the repertoire of MNP-based gene therapy platforms, targeting diverse genetic risk factors and pathological pathways.

RNA interference via siRNAs remains the most extensively explored gene therapy strategy, with several metal NPs demonstrating efficacy in silencing AD-related genes. In a study by Okła et al. (2023), PEGylated AuNPs were conjugated with siRNA targeting the APOE4 gene, a major genetic risk factor for late-onset AD. PEGylation enhanced biostability and BBB permeability, and the complexes showed successful and stable siRNA binding. The AuNP/siRNA complex demonstrated cell viability of ~75%.<sup>106</sup> Also, Lopez-Barbosa et al. (2020) developed PEGylated magnetite (Fe<sub>3</sub>O<sub>4</sub>) NPs with covalently attached BACE1 siRNA and OmpA protein (to enhance



endosomal escape). In human fibroblast and neuroblastoma cells, this platform achieved targeted BACE1 knockdown, >80% cell viability, minimal hemolysis or platelet aggregation, and high endosomal release, supporting further *in vivo* testing for siRNA gene therapy.<sup>107</sup>

Researchers have recently reported an innovative approach involving the development of Prussian blue nanocomplexes that are specifically loaded with BACE1 siRNA, metallothionein (MT), and ruthenium complexes ( $[\text{Ru}(\text{bpy})_2\text{dppz}]^{2+}$ ). This multifunctional system capitalizes on the photothermal properties of Prussian blue NPs, which, upon exposure to near-infrared (NIR) light irradiation, generate heat that facilitates the transient opening of the BBB, thereby enhancing the delivery of therapeutic agents. The BACE1 siRNA component significantly reduces the production of A $\beta$ , while the metallothionein participates in Cu<sup>2+</sup> chelation, which, in turn, synergistically inhibits A $\beta$  aggregation. Notably, the incorporation of ruthenium allows for real-time tracking of A $\beta$  degradation and aggregation processes. *In vivo* studies conducted on APP/PS1 mouse models demonstrated that this advanced platform effectively improved learning and memory functions by mitigating neuronal loss, NFTs, and glial activation through the inhibition of BACE1 activity, oxidative damage, and tau phosphorylation.<sup>108</sup>

In addition, researchers created polymeric NPs with a SPION core, carrying both siSOX9 and retinoic acid, for the control of neural stem cell differentiation in AD mice. These NPs enabled MRI, promoted neuronal differentiation, rescued memory deficits, and showed no significant toxicity *in vivo*.<sup>109</sup>

Beyond the direct gene delivery strategies discussed above, MNPs have been shown to modulate genetic pathways relevant to AD. For instance, Wang et al. (2023) demonstrated that AuNPs protect human neural stem cells from A $\beta$ -induced injury by regulating the miR-21-5p/SOCS6 pathway. AuNPs upregulated miR-21-5p expression, which in turn suppressed SOCS6, leading to



reduced tau phosphorylation, decreased apoptosis, and improved mitochondrial function.<sup>110</sup> These kinds of findings suggest that MNPs may exert neuroprotective effects through epigenetic regulation, expanding their potential therapeutic applications beyond conventional gene delivery.

Table 2 presents a summary of the research conducted on metal NPs and their potential applications in the treatment of AD. When analyzed by the intrinsic nature of the metal core, distinct therapeutic paradigms emerge. Noble metals (Au, Ag) leverage their LSPR to function as photothermal agents, using NIR light to thermally disrupt A $\beta$  fibrils, while their facile surface chemistry allows for dense functionalization with targeting ligands. In contrast, NPs with multivalent oxidation states (CeO<sub>2</sub>, Se, Mn) primarily function as potent antioxidant nanozymes, mimicking endogenous enzymes like SOD and catalase to mitigate oxidative stress and neuroinflammation, with CeO<sub>2</sub> showing particular efficacy in restoring autophagy.<sup>111</sup> Also, magnetic and semiconductor oxides, such as Fe<sub>2</sub>O<sub>3</sub>, TiO<sub>2</sub>, and RuO<sub>2</sub>, offer multimodal mechanisms. For example, iron oxide enables MRI-trackable therapy, TiO<sub>2</sub> utilizes photocatalytic effects to alter protein conformation, and ruthenium dioxide (RuO<sub>2</sub>) uniquely combines photothermal ablation with catalytic ROS clearance. Finally, the increasing use of surface engineering across all platforms, with peptides (TGN, RVG), natural compounds (resveratrol, curcumin), and polymers, highlights a convergence toward multifunctional, brain-targeted nanotherapeutics capable of crossing the BBB and modulating multiple AD pathologies simultaneously.





**Table 2.** Different types of metal NPs and their applications in the AD treatment.

Type	Characteristics	Route of Administration and Concentration	Cargo/Co-delivered Drug	Key findings	Ref.
Ag	Green synthesized, Spherical, 10-15 nm	Intraperitoneal, 2.5 mg/kg	-	Prevented the effect of deficits in recognition and spatial memory	91
	Green synthesized, spherical, 12.8-28.2 nm	Oral, 200mg/kg	-	Inhibits AChE enzyme activity and oxidative stress by increasing the levels of GSH and decreasing MDA levels	112
	Green synthesized, Spherical, 22-26 nm	In-vitro	-	Inhibition of the activity of BChE	113
	20 nm	Intraperitoneal, 2.5 mg/kg (every 48 h for 21 days)	-	Decreases tau hyperphosphorylation. increased IL-1 $\beta$ in the hippocampus. prevented oxidative stress (sulfhydryl and nitrite levels). maintained normal brain mitochondrial function. restored antioxidant status (SOD, catalase activities and GSH levels). Prevented neuroinflammation. Modulated mitochondrial function and impaired cognition	114
Au	Green synthesized, Spherical, triangular, cubic crystalline, 20 and 50 nm.	In vitro	-	Antioxidant, AChE inhibition, anti-amyloidogenic effect	115
	Spherical, ~6 nm	In vitro	functionalized with mimosine	Stabilize A $\beta$ <sub>42</sub> , trigger the disassembly of mature A $\beta$ fibres, and reduce phosphorylation of tau protein	116
	3.3 nm	Intravenous injection, 25 mg/kg, 4 weeks	stabilized with L- and D-glutathione	Inhibited aggregation of A $\beta$ <sub>42</sub> via adsorption of peptide monomers on their curvature surfaces	117
	Nanostars, 78 nm, increased to 105 nm when	1 mg/kg, injection into the caudal vein	stabilized with penetratin-loaded	Inhibited the formation of A $\beta$ fibrils as well as dissociated preformed fibrous A $\beta$ under the irradiation, neuroprotective effect on the A $\beta$ -	118



Se

		Nanoscale		
loaded with Pen peptide and Ru(II) complex			PEG and modified with Ru complex	induced cellular toxicity by applying NIR irradiation, and improved the delivery of NPs to the brain
135±5 nm	Injection in the tail vein		Coated with PEG and loaded with anthocyanin	Reduced Aβ-induced neuroinflammatory and neuroapoptotic markers via inhibiting the p-JNK/NF-κB/p-GSK3β pathway
Spherical, 70.5±6 nm.	Intravenously		Curcumin-loaded SeNPs encapsulated with PLGA nanospheres	Decreases Aβ load in the brain
Spherical, 100 nm	In vitro (PC12)		Conjugated with LPFFD and TGN	Suppress extracellular Aβ fibrillation by disrupting hydrophobic and electrostatic interactions, and suppress the Aβ fibre-mediated generation of ROS
14 nm	PC12 cell, and Muse model, Oral administration		Conjugated with Resveratrol and functionalized with TGN peptide	Decreased Aβ aggregation and Aβ-induced ROS, while increasing activity of antioxidation enzymes, down-regulating Aβ-induced neuroinflammation via the NFκB/mitogen-activated protein kinase/Akt signal pathway
Spherical, 60-90 nm	Oral (100 mg/kg/day for 60 days)		Resveratrol	Clearance of Aβ and deactivation of tau hyperphosphorylation, Regulation of Sirt1/miRNA-134/GSK3β expression
Spherical, ≥50 nm	Oral		Combined with adipose-derived mesenchymal stem cells (AMSCs) transplant	Synergistic effects: Reduced the deposition of Aβ and increased the concentration of BDNF
Spherical, 25 and 29 nm	In vitro		Stabilized with Epigallocatechin gallate, coated with TET-1 peptide	Inhibited Aβ fibrillation and disaggregated preformed Aβ fibrils



	Spherical, 86 nm to 95 nm	In vitro	modified with Sialic acid (SA) and coated with B6 peptide	Inhibited A $\beta$ aggregation, and disaggregated preformed A $\beta$ fibrils	124
	Spherical, 89 $\pm$ 4.5 nm	In vitro (SH-SY5Y)	Allied with chondroitin sulfate	Inhibited A $\beta$ aggregation and A $\beta$ -induced cytotoxicity, decreased okadaic acid-induced actin cytoskeleton instability, decreased ROS and MDA and increased GSH-Px, attenuated the hyperphosphorylation of tau (Ser396/Ser404) by regulating the expression of GSK-3 $\beta$	95
<b>Ru</b>	Spherical, 5 nm, the whole structure 80 nm	SH-SY5Y and Intravenous injection, 1 mg/kg, 5 weeks	Coated RVG or NGF peptides	Owing to their photothermal properties, these NPs effectively inhibited the aggregation of A $\beta$ and disaggregates A $\beta$ fibrils suppress extracellular A $\beta_{40}$ self-assembly and Zn <sup>2+</sup> -induced fibrillization. suppress the Zn <sup>2+</sup> -Ab <sub>40</sub> mediated generation of ROS and their neurotoxicity	125
	Spherical, 35 nm	In vitro (PC12)	L-Cys modified	Cleared A $\beta$ and ROS, restored mitochondrial autophagy and normalized mitochondrial dysfunction, regulated microglia polarization, inhibited microglia overactivation, and relieved neuroinflammation	99
<b>RuO<sub>2</sub></b>	Spherical, 5 nm	RuO <sub>2</sub> (0.5 mg/kg), tail vein injection	ICG-labelled		100
<b>ZnO</b>	Green synthesized, Irregular, small spherical, narrow particles included in hexagonal structures with a size ranging from 2.23 to 49.56 nm.	In vitro	-	AChE inhibitory activity	98
<b>TiO<sub>2</sub></b>	Thin films	In vitro	-	Caused conformational change of A $\beta$ . The loss in the crucial structure of A $\beta$ leads to a reduction in the fibril formation (thought to be induced through a photocatalytic process)	126



<b>Fe<sub>2</sub>O<sub>3</sub></b>	20 nm	Intraperitoneal and intra-hippocampal, 0.01-0.1 μg/kg-1, 4 days, each day before the MWM test	Coated with PEG 3000	Inhibited Aβ aggregation and facilitated learning and memory deficit. Enhanced level of hippocampal proteins (BDNF, p-CREB, STIM1 and STIM2)	127
	21±3.5 nm	Intracranial, 2 mg/ml, 10 μg bound fibrin per injection	Conjugated with Fibrin γ377-395 peptide	Reduced microglial cell activation and reduced the tau pathology in old mice	128
<b>CeO<sub>2</sub></b>	Spherical, 20 -25 nm	Oral, for one month, at 1 mM concentrations	-	Restored the activity of SOD, affected the climbing activity of elav; htau flies, elicited a significant decrease in hTau gene expression and increased the mRNA expression of key autophagy genes ATG1 and ATG18 (replenishing the levels of SOD and tau clearance via the activation of autophagy)	111
	Spherical, 3 nm	Unilateral subicular injections	Conjugated with triphenylphosphonium	Mitigated reactive gliosis and morphological mitochondrial damage Effectively crosses the BBB, reduces oxidative stress (through the Nrf-2/HO-1 signaling pathway), inhibits Aβ aggregation, and promotes the recovery of neurological function	129
<b>Mn-doped CeO<sub>2</sub></b>	Approximately 120 nm	Tail vein injection	Loaded with Resveratrol	Eliminated toxic metallic ion, decreased oxidative stress, and promoted neurite outgrowth	92
<b>CeNP@ MnMoS<sub>4</sub></b>	Core-Shell, Approximately 5 nm	in vitro			93

Abbreviations:

Ag: Silver, GSH: Glutathione, MDA: Malondialdehyde, Au: Gold, IL-1 β: Interleukin 1 beta, SOD: Superoxide dismutase, Se: Selenium, ROS: Reactive oxygen species, BDNF: Brain-derived neurotrophic factor, Ru: Ruthenium, RuO<sub>2</sub>: Ruthenium dioxide, ZnO: Zinc oxide, TiO<sub>2</sub>: Titanium dioxide, Fe<sub>2</sub>O<sub>3</sub>: Iron(III) oxide, PEG: Polyethylene glycol, CeO<sub>2</sub>: Cerium dioxide, Mn: Manganese, BBB: Blood-brain barrier

**Fig. 6** illustrates the complex mechanistic landscape through which various MNPs exert their therapeutic effects in the management of AD. While many facets of these interactions remain to be fully elucidated, the current literature suggests a multifaceted pharmacological profile, which can be synthesized into several key pathways:

First, MNPs demonstrate significant anti-amyloidogenic properties by targeting A $\beta$  at multiple stages. This includes inhibiting the initial aggregation of A $\beta$  monomers, promoting the disaggregation of established fibrils, and facilitating photothermal degradation. Furthermore, these NPs enhance A $\beta$  clearance and induce conformational changes that mitigate toxicity. Parallel to this, anti-tau mechanisms are activated, characterized by the inhibition of tau hyperphosphorylation, reduction of overall tau pathology, and the downregulation of tau gene expression. Also, a cornerstone of MNPs therapy lies in their antioxidant and neuroprotective capabilities. By mimicking endogenous enzymes, such as SOD and Catalase, and activating the Nrf2/HO-1 signaling pathway, MNPs effectively scavenge ROS, restore GSH levels, and safeguard mitochondrial integrity. This is closely linked to the suppression of neuroinflammation, where MNPs modulate microglia polarization and inhibit pro-inflammatory cascades, specifically the p-JNK/NF- $\kappa$ B/p-GSK3 $\beta$  and MAPK/Akt pathways.

Beyond above mentioned pathways, MNPs serve as potent enzyme inhibitors, targeting AChE and butyrylcholinesterase (BChE) to enhance cholinergic neurotransmission. They also play a critical role in restoring metal ion homeostasis by chelating excess ions and suppressing the fibrillization induced by Cu $^{2+}$ , Fe $^{2+}$ , and Zn $^{2+}$ . Finally, the therapeutic scope of MNPs extends to genetic and cellular regulation; they stimulate autophagy-related genes, modulate the Sirt1/miRNA-134/GSK3 $\beta$  axis, and enhance the expression of neurotrophic factors such as BDNF and p-CREB, alongside calcium-sensing proteins like STIM1 and STIM2.



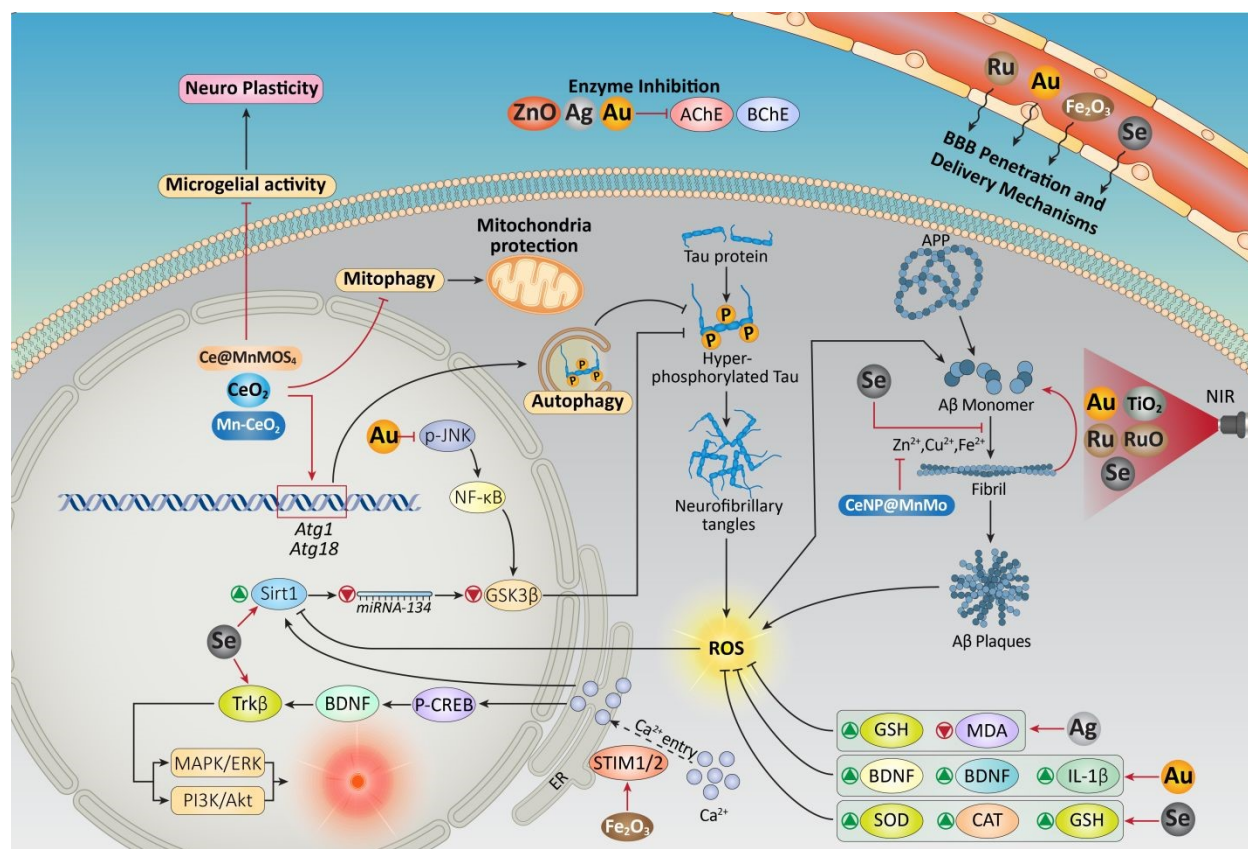


**Fig. 6** Schematic representation of the multifaceted therapeutic mechanisms of various metal NPs in AD management. NPs such as Ru, Au, Fe<sub>2</sub>O<sub>3</sub>, and Se facilitate effective BBB crossing for targeted delivery. Amyloid- $\beta$  (A $\beta$ ) and Tau modulation: Se and CeNP@MnMo inhibit A $\beta$  fibrillization and metal-induced aggregation, while Au, TiO<sub>2</sub>, Ru, and RuO promote A $\beta$  degradation via NIR PTT. Au further inhibits p-JNK signaling to reduce Tau hyperphosphorylation and NFTs. Enzyme inhibition and neuroplasticity: ZnO, Ag, and Au act as potent inhibitors of AChE and BChE. Se enhances neuroplasticity by activating the Sirt1/Trk $\beta$ /BDNF signaling axis. Autophagy and organelle protection: Cerium-based NPs regulate autophagy/mitophagy pathways and Fe<sub>2</sub>O<sub>3</sub> modulates STIM1/2 for calcium homeostasis and mitochondrial protection. Antioxidant and anti-inflammatory effects: Ag, Au, and Se significantly attenuate oxidative stress and neuroinflammation by restoring antioxidant enzymes (SOD, CAT, GSH), reducing MDA levels, and downregulating pro-inflammatory cytokines like IL-1 $\beta$ .

## 7. Alzheimer's theranostic potential of metallic NPs

The advent of nanotechnology and the conceptual emergence of theranostics, a combination of “therapy” and “diagnostics”, offer a paradigm shift in the diagnosis and treatment of AD. Theranostic platforms are defined by their unique capability to integrate diagnostic and therapeutic functions within a single nanoscale construct. These multifunctional NPs are engineered to deliver



therapeutic payloads to pathologic foci, enable real-time disease monitoring through various imaging modalities, and provide feedback on drug distribution and efficacy. Such dual-action platforms represent a step towards precision and personalized medicine by facilitating early diagnosis, targeted treatment, and dynamic adjustment of therapeutic regimens in response to disease evolution.<sup>130</sup>

Metallic NPs, including Au, Fe<sub>3</sub>O<sub>4</sub>, CeO<sub>2</sub>, Ru, Se, and ZnO, are particularly well-suited for theranostic applications due to their unique optical, magnetic, electronic, and catalytic properties. These NPs possess the ability to be functionalized with biomolecules for targeted delivery, conjugated with imaging agents for multimodal detection (fluorescence, MRI, PET, single-photon emission computed tomography (SPECT)), and tailored for controlled drug release or phototherapeutic modalities such as PTT and photodynamic therapy (PDT).<sup>131,132</sup> Nanotheranostics not only facilitate early and sensitive detection of AD-specific molecular aberrations (A $\beta$  plaques, tau aggregates, metal ion dyshomeostasis, and oxidative milieu) but also enable efficient CNS delivery of neuroprotective, anti-amyloid, and anti-inflammatory agents while minimizing systemic toxicity.<sup>133,134</sup>

From the perspective of clinical need, the goal of such platforms is threefold: 1) to overcome the poor brain penetrance of drugs by exploiting the small size, modifiable surfaces, and receptor-mediated transport mechanisms of NPs; 2) to provide comprehensive in vivo imaging for early disease diagnosis and longitudinal monitoring of pathological progression or therapeutic response; and 3) to deliver drugs, genes, or biological modifiers that directly interfere with AD pathologies in situ with minimal off-target effects. Importantly, theranostic metallic NPs can be tailored for patient-specific interventions by integrating molecular biomarkers into their design, advancing the promise of precision medicine in the context of AD.<sup>135</sup>



AuNPs have become the most extensively studied theranostic agents in AD due to their high biocompatibility, ease of surface modification, adjustable optical properties, and strong ability to cross the BBB. For example, as depicted in **Fig. 7**, Morales-Zavala et al. (2021) developed a neurotheranostic nanosystem based on Au nanorods (called GNRs) that functions as a therapeutic peptide delivery system and can be detected *in vivo* by  $\mu$ -CT, serving as a diagnostic tool. GNRs functionalised with the peptides Ang2 (a shuttle to the CNS) and D1 (which binds to the A $\beta$  peptide and inhibits its aggregation) enabled the detection of differences *in vivo* between wild-type and AD mice (APP<sup>swe</sup>/PSEN1<sup>dE9</sup>) 15 minutes after a single dose via  $\mu$ -CT. Notably, based on their outcomes,  $\mu$ -CT signals were higher in animals treated with GNRs-D1/Ang2 than in those treated with GNRs-Ang2. Furthermore, after recurrent treatment for over one month with GNRs-D1/Ang2, a reduction in amyloid load and inflammatory markers in the brain was observed. Thus, this newly designed nanosystem shows promising properties for neurotheranostics of AD.<sup>136</sup>

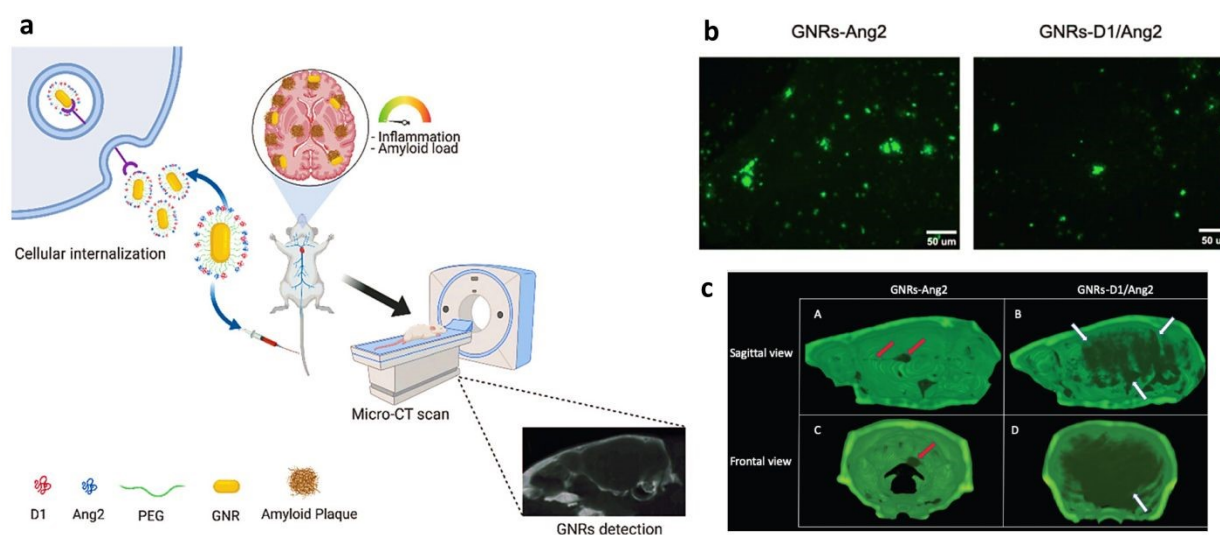


**Fig. 7** Evaluation of cell penetration, brain delivery, amyloid plaque attachment and *in vivo* detection by  $\mu$ -CT of Au nanorods (GNRs)-D1/Ang2 (a). Representative image of cortex brain slices of animals treated with the GNRs-Ang2 and GNRs-D1/Ang2 nanosystems, showing the effects of GNRs-D1/Ang2 on reducing the amyloid load in the brain (b). Images of the skull by  $\mu$ -CT of transgenic APP<sup>swe</sup>/PSEN1<sup>dE9</sup>



mice treated for one month with 100  $\mu$ L of GNRs-D1/Ang2 or GNRs-Ang2 10 nM. cA and cB show a sagittal section of a transgenic mouse treated with GNRs-Ang2 and GNRs-D1/Ang2, respectively. Also, cC and cD show the frontal section of a transgenic mouse treated with GNRs-Ang2 and GNRs-D1/Ang2, respectively. The white arrows indicate the accumulation of AuNPs in the amyloid aggregates. The red arrows indicate the accumulation of AuNPs in the circulation. Reproduced with permission from <sup>136</sup>.

Additionally, in a recent study, Huang et al. (2023) encapsulated bexarotene and AgAuSe quantum dots within Lamp2b-RVG-overexpressed neural stem cell membranes. This design leveraged the RVG peptide's affinity for neuronal acetylcholine receptors, along with the innate brain-homing and immune-evasive properties of stem cell membranes. Using NIR-II imaging, they tracked the particles' passage from blood circulation into the brain and down to single neurons in real time. Additionally, as they reported, in an Alzheimer's mouse model, a single intravenous dose delivering only 0.5% of the standard oral bexarotene amount drove a significant rise in ApoE levels and cut  $\beta$ -amyloid concentrations in the brain interstitial fluid by about 40%. Over a month of treatment, amyloid plaque accumulation was halted entirely, neurons were protected from A $\beta$ -induced apoptosis, and the mice maintained normal performance on cognitive tasks (**Fig. 8**).<sup>137</sup>



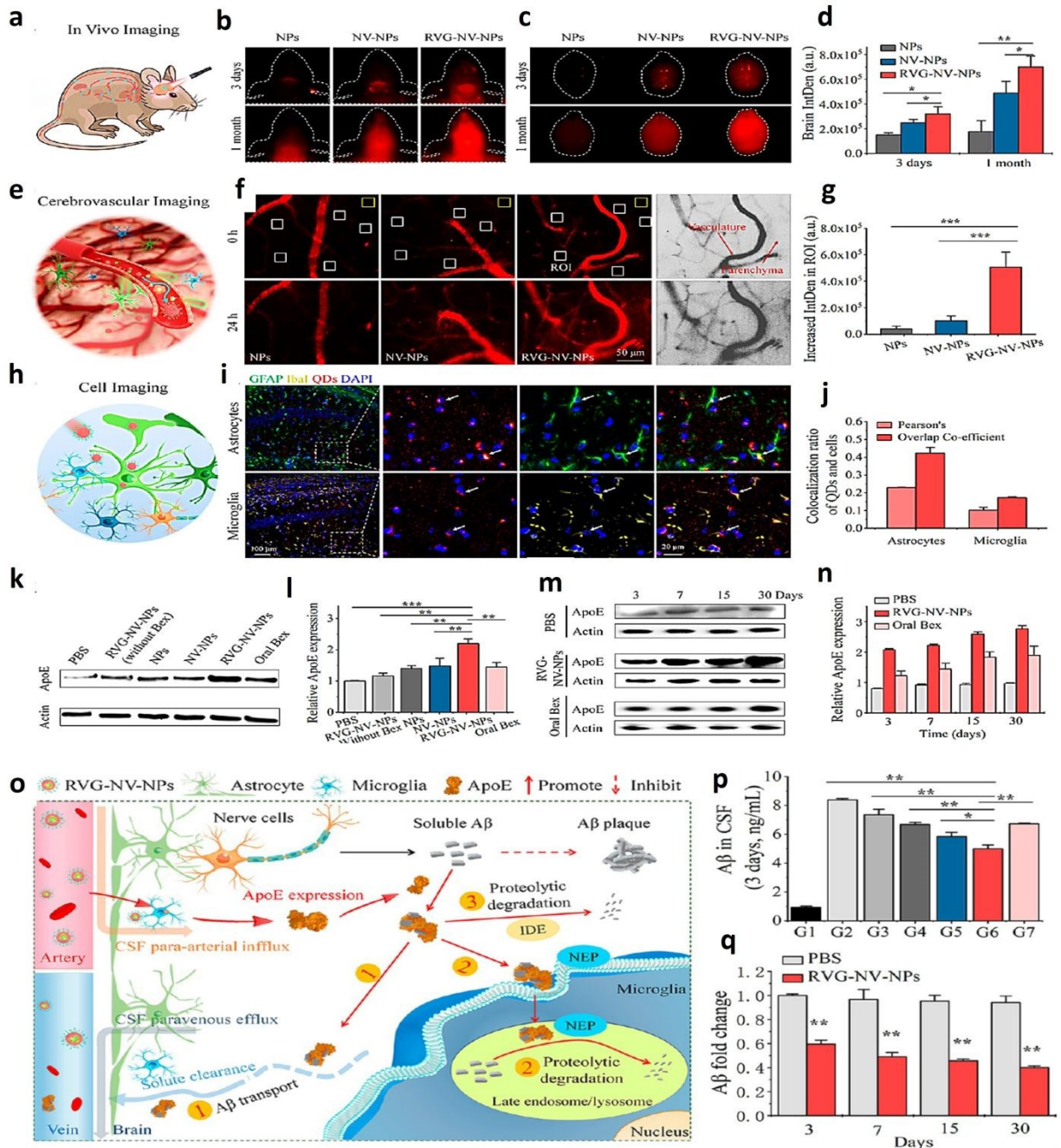


**Fig. 8** *In vivo* brain delivery assay of RVG-NV-NPs in APP/PS1 mice by the multiscale NIR-II imaging. (a) Schematic illustration of *in vivo* imaging of brain delivery of nanoformulation. (b) *In vivo* imaging of heads of living mice using the NIR-II fluorescence of AgAuSe QDs. (c) Representative fluorescence images of the mouse brains in NPs, NV-NPs, and RVG-NV-NPs groups at days 3 and 30 after injection. (d) Quantitative data of (c). IntDen: integrated density. (e) Schematic illustration of *in vivo* mesoscopic imaging of cerebrovascular. (f) *In vivo* fluorescence imaging of the penetration of RVG-NV-NPs from the blood



vessel to the brain parenchyma. (g) Enhanced fluorescence intensities in the regions of interest (ROI, the white boxes) in (f) from 0 to 24 h p.i. (h) Schematic illustration of cell imaging. (i) Representative fluorescence images of QDs and microglia or astrocytes in brain sections of the hippocampus from mice. (j) Pearson's correlation and overlap coefficient assay between QDs and microglia or astrocytes in the mouse brain images from (i). (k) ApoE expression in hippocampus quantified by WB assay. (l) Quantification of (k). (m) WB assay of ApoE expression in the hippocampus of mice at days 3, 7, 15, and 30 after treatment. (n) Quantification of (m). (o) Schematic illustration of RVG-NV-NPs nanoformulation-mediated ApoE expression and soluble A $\beta$  clearance via A $\beta$ -binding ApoE isoform. Soluble A $\beta$  can be cleared via ApoE-dependent CSF paravenous efflux and proteolytic enzymes (including NEP and IDE). (p) ELISA assay of A $\beta$  in the CSF of mice at day 3. (q) ELISA assay of A $\beta$  in the CSF of PBS-treated or RVG-NV-NPs-treated mice at days 3, 7, 15, and 30. Reproduced with permission from <sup>137</sup>.

## 8. Safety, toxicity, and biocompatibility

The utilization of metal NPs in the field of medicine necessitates a thorough evaluation of their safety and biocompatibility, which are influenced by factors such as particle size, surface chemistry, route of administration, and clearance mechanisms. Numerous MNPs have demonstrated therapeutic potential; however, they may also present neurotoxic effects under specific conditions. Emerging epidemiological evidence indicates that human exposure to certain nanosized materials present in the environment may contribute to the onset and/or progression of AD.<sup>138</sup> It is essential to elucidate the cellular and molecular mechanisms through which NPs may exert adverse effects on neuronal health and contribute to the pathology associated with AD.

### 8.1. Oxidative and cellular damage

Ironically, the same particles that can reduce oxidative stress at one dose might trigger oxidative stress at a higher dose or if improperly engineered. MNPs can catalyze the production of ROS by interacting with cellular metabolites. For example, metal oxide NPs, such as Fe<sub>3</sub>O<sub>4</sub>, CuO, cobalt oxide (CoO), and TiO<sub>2</sub>, can generate free radicals *in vivo*; metal ions released from NPs (Fe<sup>2+</sup>,



Cu<sup>+</sup>) can participate in Fenton chemistry to produce hydroxyl radicals.<sup>3</sup> Excess ROS from NPs leads to the oxidation of proteins and lipids in neurons, as evidenced by the induction of oxidative stress and an impairment of the antioxidant enzyme glutathione peroxidase in the rat brain following AuNPs injection (20 nm, 20 µg/kg body weight). AuNPs also cause the generation of 8-hydroxydeoxyguanosine (8-OHdG), caspase-3 and heat shock protein 70 (Hsp70), and IFN-γ, which may lead to inflammation and DNA damage/cell death.<sup>139</sup> Mitochondria are sensitive targets; NP-induced ROS cause mitochondrial dysfunction, drop ATP levels, and can trigger apoptosis via caspase activation. DNA damage has also been observed (e.g. oxidative DNA breaks or chromatin fragmentation) in cells treated with high concentrations of some MNPs.<sup>26</sup> This cellular damage cascades into neurodegeneration if not controlled.

## 8.2. Size, shape, and surface effects

The physical characteristics of NPs strongly influence toxicity. Smaller particles generally penetrate biological membranes more easily and can reach intracellular organelles, potentially disrupting them. For instance, AuNPs in the 1-2 nm range were found to cross the BBB by disrupting endothelial tight junctions, accumulating in brain parenchyma and causing more toxicity than larger gold particles.<sup>140</sup> NPs' shape strongly influences biological interactions and toxicity. It has been revealed that anisotropic forms (rods, wires, plates) typically present larger surface areas and sharp edges that increase membrane disruption, protein adsorption, and cellular uptake compared with compact spheres, often leading to higher cytotoxicity and inflammatory responses.<sup>141,142</sup> Surface charge is another influential factor. Highly cationic NPs are more likely to be taken up by cells (which can be good for delivery), but also can nonspecifically damage cell membranes and proteins, and activate the complement system.<sup>143</sup> These findings underscore that by tuning NPs' size/shape, one can mitigate some toxic effects. Smooth, intermediate-size (10-50



nm) particles with neutral or slight negative charge tend to be the most biocompatible in the brain, whereas extremely small, highly charged, or oddly shaped particles pose higher risks.<sup>144,145</sup>

### **8.3. Immune response and biocompatibility**

The interaction of NPs, in particular metal NPs, has been well-documented.<sup>146,147</sup> The body's immune system often recognizes unmodified metal NPs as foreign invaders. Phagocytic cells (microglia in the CNS, macrophages elsewhere) will engulf NPs, which can lead to inflammation. The persistent presence of NPs can also form granulomas or deposits in reticuloendothelial organs (liver, spleen).<sup>148</sup> In this regard, surface functionalization has a significant impact on immune compatibility. As noted earlier, PEGylation can reduce opsonisation by serum proteins, thereby conferring stealth properties to NPs.<sup>149</sup> Biocompatibility testing has revealed that naked MNPs are quickly sequestered by phagocytes, reducing their therapeutic availability and potentially causing local immune activation.<sup>150</sup> So far, many MNPs have shown acceptable safety in animals when properly coated and dosed, but careful dose-escalation studies are needed before human use. Importantly, chronic exposure studies are lacking. If patients were to receive NP treatments repeatedly or have NPs lingering in the brain for years, we need to ensure no late-emerging toxicity or interference with brain metabolism.

### **8.4. Metal ion release and long-term fate**

Some metal NPs (especially oxides) may dissolve or corrode over time in the body, releasing metal ions. These ions (e.g. Ag<sup>+</sup> from AgNPs, Zn<sup>2+</sup> from ZnO, Fe<sup>2+</sup> from SPIONPs) can contribute to toxicity if they accumulate. For example, excessive release of silver ions leads to oxidative stress and can interfere with enzymes. IONPs might increase the labile iron pool in the brain; iron accumulation is itself a risk factor for neurodegeneration. Excessive Zn<sup>2+</sup> can induce tau aggregation and also activate key kinases that hyperphosphorylate tau. This ion may also impair



the activity of the enzyme that normally dephosphorylates tau, thereby leading to tau accumulation.<sup>13</sup> On the other hand, a controlled slow release might be beneficial if the body can incorporate or excrete the ions safely (for instance, iron from SPIONPs can be stored by ferritin and eventually recycled, and zinc from ZnO NPs can be bound by metallothioneins or excreted).<sup>151</sup> The degradation products of NPs need to be non-toxic. Au, for example, does not break down into ions under physiological conditions (Au<sup>0</sup> stays elemental), which means AuNPs could potentially persist indefinitely if not cleared by cells. Studies in rodents have found traces of AuNPs in the liver, spleen, and brain months after injection<sup>152</sup>. While inert, their long-term presence is an unknown; could they affect microcirculation or cell function over the years? These are questions regulators will ask.

### **8.5. Mitigation strategies**

Researchers are proactively addressing these safety issues. One approach is to co-administer antioxidants or develop antioxidant surfaces to prevent NPs-induced ROS. In fact, one study showed that delivering N-acetylcysteine alongside MNPs reduced oxidative markers and protected neurons.<sup>153</sup> Many MNPs themselves (such as Au, Se, Ce, ZnO) possess inherent antioxidant properties and are considered safer in AD models for that reason.<sup>154</sup> Using biogenic or green synthesis approaches produces NPs coated with biological molecules that often neutralise any residual reactivity. Green-synthesised Ag and AuNPs exhibited less neurotoxicity and even an extra antioxidant effect compared to chemically synthesised ones.<sup>30,155</sup> Additionally, to prevent unintended interactions, thorough characterization and standardisation of NPs is vital (size distribution, zeta potential, purity, etc.), as minor variations can alter toxicity. Regulatory agencies are beginning to draft guidelines for testing nanomaterials, emphasising comprehensive *in vitro* and *in vivo* toxicity assays, including neurotoxicity, immunotoxicity, and genotoxicity evaluations.



Despite promising preclinical and early clinical research, as of September 2025, there are no FDA-approved metal nanoparticle-based products largely because preclinical safety testing is still ongoing and optimal designs are being refined. The encouraging news is that several MNPs have shown windows of safe and effective dosing in animal models, such as selenium, Au, ruthenium, and ZnO NPs, which have been noted as relatively safe at therapeutic doses in AD models. Nonetheless, translating these to humans will require confirming that they do not cause significant inflammation, off-target organ damage, or cognitive side effects over the long term.

### **8.6. Comparative overview of metal NP platforms**

Given the diversity of metal NPs explored for AD therapy, a comparative understanding of their relative advantages and limitations is essential for informed platform selection. Based on the studies reviewed in Table 2 and the safety considerations discussed above, the following comparative profile emerges.

AuNPs offer exceptional versatility due to their ease of functionalization, tunable plasmonic properties for PTT, and generally inert core. Their advantages include multifunctional surface chemistry and high biocompatibility in the 10-50 nm size range. Likewise, Ru-based NPs, including RuNPs and RuO<sub>2</sub>NPs, represent an emerging class with bifunctional capabilities: photothermal ablation of A $\beta$  aggregates combined with intrinsic ROS scavenging.<sup>100,125</sup> Alongside their advantages, the limitations of AuNPs include poor biodegradability (persisting indefinitely in tissues) and potential for dose-dependent neuroinflammation, as evidenced by increased IL-1 $\beta$  and caspase-3 activation.<sup>114,139</sup> In addition, ultrasmall AuNPs (<3 nm) raise toxicity concerns due to enhanced BBB penetration and nonspecific accumulation.<sup>140</sup> RuNPs are novel, and their long-term toxicity data and biodistribution profiles in mammals remain limited compared to more established platforms like Au or Se.



SeNPs are distinguished by their dual role as antioxidant nanozymes and essential nutritional elements. They demonstrate potent ROS scavenging, inhibition of A $\beta$  aggregation, and excellent biocompatibility, particularly when green-synthesized or functionalized with natural compounds like resveratrol.<sup>121–83</sup> Likewise, CeO<sub>2</sub> NPs are among the most potent catalytic antioxidants, leveraging their multivalent Ce<sup>3+</sup>/Ce<sup>4+</sup> redox cycling to mimic SOD and catalase. They are particularly effective against neuroinflammation and mitochondrial damage.<sup>111,129</sup> However, the SeNPs' main limitation lies in the narrow therapeutic window; excessive degradation can release selenite ions, which may be toxic at high concentrations. Also, the CeONPs efficacy is highly dependent on the Ce<sup>3+</sup>/Ce<sup>4+</sup> ratio and crystallite size, leading to batch-to-batch variability. Long-term accumulation in the brain and reticuloendothelial organs remains a concern.

Iron oxide NPs offer the unique advantage of MRI traceability, enabling theranostic applications. They have shown efficacy in reducing A $\beta$  pathology and enhancing synaptic proteins (BDNF, p-CREB).<sup>127</sup> Yet, the primary disadvantage is the potential release of iron ions, which could contribute to the labile iron pool and exacerbate oxidative stress via Fenton chemistry, a particular concern given iron dyshomeostasis in AD.

Ag, ZnO, and TiO<sub>2</sub> NPs, while showing anti-amyloidogenic and enzyme-inhibitory effects in vitro, raise greater safety concerns. AgNPs are prone to dissolution and Ag<sup>+</sup> release, leading to oxidative stress and potential mitochondrial damage.<sup>91,112</sup> ZnO and TiO<sub>2</sub> NPs can generate ROS under physiological conditions, and their chronic neurotoxicity profiles are less favorable than those of Au, Se, or CeO<sub>2</sub>.<sup>98,126</sup>

In summary, selecting an MNP platform involves trade-offs among therapeutic efficacy, biocompatibility, biodegradability, and multifunctionality. While noble metals such as Au offer versatility and surface flexibility, redox-active nanozymes such as Se and CeO<sub>2</sub> provide intrinsic



antioxidant defence. Emerging platforms such as RuO<sub>2</sub> are expanding the therapeutic toolkit, but rigorous head-to-head comparative studies under standardised conditions remain urgently needed to guide clinical translation. Table 3 presents a side-by-side comparison of the major metal NP platforms, highlighting their relative strengths, limitations, and suitability for different therapeutic applications in AD.

**Table 3.** Comparison of metal NP platforms: primary applications, advantages, limitations, and representative references.

NP type	Key advantages	Key disadvantages/limitations	Best suited for
Au	Easy functionalization, photothermal capability, inert core	Non-biodegradable, potential chronic accumulation, dose-dependent inflammation	Drug delivery, PTT, multifunctional platforms
Se	Antioxidant nanozyme, essential nutrient, good biocompatibility	Narrow therapeutic window, potential selenite toxicity	ROS scavenging, neuroprotection, combination therapy
CeO <sub>2</sub>	Potent SOD/catalase mimetic, anti-inflammatory	Batch variability (Ce <sup>3+</sup> /Ce <sup>4+</sup> ratio), long-term accumulation concerns	Oxidative stress, mitochondrial protection, neuroinflammation
Fe <sub>2</sub> O <sub>3</sub>	MRI traceability, theranostic potential	Iron release (Fenton chemistry), concerns in iron dyshomeostasis	Imaging-guided therapy, tracking BBB penetration
Ru/RuO <sub>2</sub>	Bifunctional (photothermal + antioxidant), emerging platform	Limited long-term safety data, preclinical stage	Combined photothermal and antioxidant therapy
Ag, ZnO, TiO <sub>2</sub>	Anti-amyloidogenic, enzyme inhibition	Higher toxicity risk, ion release, ROS generation	In vitro mechanistic studies (caution for in vivo)

## 9. Future perspectives and challenges

The translation of metal NP platforms from preclinical research to clinical AD management will require a shift from general concepts to specific, actionable strategies across three key areas, including nanomaterial design, therapeutic integration, and clinical translation.



*Nanomaterial surface engineering:* The next generation of MNPs must move beyond basic functionalization toward precision-engineered surfaces. Key priorities include 1) ligand selection and density optimization: identifying brain-targeting ligands (TGN, RVG, transferrin) with optimal surface densities to maximize receptor-mediated transcytosis while minimizing immunogenicity. 2) Stimuli-responsive coatings: Developing surface chemistries that respond to disease-specific microenvironments, such as ROS-cleavable polymers, pH-sensitive linkers, or enzyme-triggered release mechanisms, to confine therapeutic activity to amyloid plaques or neuroinflammatory sites. 3) Biomimetic functionalization: Exploring patient-derived coatings (erythrocyte or neural stem cell membranes) to reduce immune clearance and enhance biocompatibility, moving toward personalized nanocarriers.

*Hybrid and multifunctional systems:* Single-function NPs are unlikely to address AD's complex pathology. Future platforms should integrate multiple therapeutic and diagnostic modalities, including 1) Combination therapy carriers: Designing NPs that co-deliver synergistic agents, such as anti-amyloid peptides with antioxidant nanozymes, or BACE1 siRNA with metal chelators, to simultaneously target protein aggregation, oxidative stress, and genetic risk factors. 2) Theranostic integration: Embedding imaging reporters (MRI-detectable iron oxide cores, NIR-II fluorescent dyes, or ruthenium complexes) alongside therapeutic cargo to enable real-time tracking of biodistribution, target engagement, and therapeutic response. 3) Multifunctional core-shell architectures: Developing composite NPs (Prussian blue cores with polymer shells or metal-organic frameworks) that combine photothermal capacity, drug loading, and stimuli-responsive release within a single platform.

*Clinical translation pathways:* Moving from bench to bedside demands a clear, phased roadmap: 1) Manufacturing scalability: Establishing reproducible, good manufacturing practice (GMP)-



compliant synthesis protocols for monodisperse NPs with batch-to-batch consistency in size, surface chemistry, and functionalization density. 2) Regulatory harmonization: Engaging with regulatory agencies early to define acceptable characterization assays, toxicity endpoints, and biodistribution standards specific to nanomedicines. 3) Route-of-delivery optimization: Systematically comparing intravenous, intranasal, and focused ultrasound-assisted delivery to identify the safest and most effective route for different MNP platforms and patient populations. 4) Long-term safety assessment: Conducting chronic toxicity studies in relevant animal models to evaluate NP fate in brain tissue, potential off-target accumulation, and effects on cognition and neuroinflammation over clinically relevant timescales. 5) Patient stratification: Integrating rapid, multiplexed diagnostic platforms (SERS-based blood tests) to identify patients most likely to benefit from specific MNP formulations based on their molecular and genetic profiles (APOE4 status, predominant pathology).

By pursuing these specific strategies, precision surface engineering, hybrid system development, and structured clinical pathways, the field can accelerate the translation of metal NP technologies from promising preclinical demonstrations into meaningful clinical interventions for Alzheimer's disease.

## 10. Conclusion

Metal NPs offer an innovative and versatile strategy for addressing AD. As this review shows, MNPs have proven capable of intervening in key pathological processes of AD, from preventing A $\beta$  aggregation and tau phosphorylation to reducing oxidative stress and ferrying drugs through the BBB. Au, Ag, Se, CeO<sub>2</sub>, ZnO, Fe<sub>3</sub>O<sub>4</sub>, and Ru NPs (among others) have all demonstrated



neuroprotective effects in preclinical models, enhancing both biochemical and behavioral outcomes. These particles can function as both therapeutic agents and diagnostic tools, embodying the theranostic concept that is particularly appealing for a complex disease like AD. Moreover, the flexibility of nanotechnology enables a single NP platform to target multiple aspects of the disease, which is especially advantageous given AD's intertwined pathologies.

However, it is equally apparent that MNPs are a “double-edged sword.” They may also exhibit neurotoxic effects if not carefully engineered, with factors such as size, shape, and coating influencing whether a NP aids or harms. The contrasting findings of neuroprotection versus neurotoxicity highlight a fundamental conclusion: the ultimate impact of a metal NP in the brain depends on its design and biological interactions. Therefore, an important focus for future research is to develop a comprehensive structure-activity relationship for MNPs, linking their physicochemical properties with safety and efficacy outcomes. This will inform the optimization of NPs to maximize therapeutic benefits while reducing side effects.

Encouragingly, ongoing advances in NP surface engineering, targeting ligands, and responsive drug release are addressing many initial safety concerns. Several types of MNPs (e.g., formulations of Au, Se, Ru, ZnO) are already reported to be safe and effective in AD animal studies at therapeutic doses. Simultaneously, the field is moving towards established best practices for characterization and biocompatibility testing, paving the way for regulatory approval. It must be acknowledged that, to date, no metal nanoparticle-based therapy has entered clinical trials for AD. The journey from laboratory research to clinical application will require continued interdisciplinary collaboration and likely iterative refinement of nanomedicines. However, the potential rewards are substantial. If even a fraction of the preclinical successes translates to humans, metal NPs could address critical gaps in AD treatment, such as removing toxic proteins



that antibodies alone cannot clear or safeguarding neurons from ongoing oxidative and inflammatory damage, thereby helping preserve cognitive function. They could also revolutionise AD diagnosis, enabling early detection of pathology and precise monitoring of therapeutic response.

In summary, MNPs provide a powerful toolkit to combat AD on multiple levels. They signify a shift from the traditional “one-drug, one-target” approach towards a multifunctional, targeted, and possibly personalized strategy. While challenges remain, current research offers an optimistic message: with meticulous design and rigorous testing, these nanotechnologies may ultimately bring about significant improvements in the lives of patients with AD.

## Declarations

**Competing Interests:** The authors have no relevant financial or non-financial interests to disclose.

**Funding:** The authors did not receive support from any organization for the submitted work.

**Authors' Contribution and Agreement:** **Sadegh Khorrami** conceived the study, developed the methodology, carried out the investigations, and wrote the original draft. **Atena Alifarsangi** contributed to the study conception, helped design the methodology, and co-wrote the original draft. **Layth Jasim Mohammed** performed the formal data analysis and took part in the experimental investigations. **Ahmed M. Amshawee** conducted formal analyses and contributed to the investigative work. **Ali Zarrabi** supervised the project and handled writing for review and editing. All authors have seen and approved the final version of the manuscript being submitted. They warrant that the article is the authors' original work, hasn't received prior publication and isn't under consideration for publication elsewhere.



***Ethics Approval:*** Not applicable

***Data, Material and/or Code Availability:*** Not applicable

**Consent to Participate:** Not applicable

**Consent for Publication:** Not applicable



## References

- 1 J. Zhang, Y. Zhang, J. Wang, Y. Xia, J. Zhang and L. Chen, *Signal Transduct. Target. Ther.*, 2024, **9**, 211.
- 2 E. Asimakidou, J. K. S. Tan, J. Zeng and C. H. Lo, *Pharmaceuticals*, 2024, **17**, 612.
- 3 A. Behera, N. Sa, S. P. Pradhan, S. Swain and P. K. Sahu, *J. Alzheimer's Dis. Reports*, 2023, **7**, 791.
- 4 C. I. P. Chaparro, B. T. Simões, J. P. Borges, M. A. R. B. Castanho, P. I. P. Soares and V. Neves, *Pharmaceutics*, 2023, **15**, 2316.
- 5 S. Fakhri, S. Abdian, S. N. Zarneshan, S. Z. Moradi, M. H. Farzaei and M. Abdollahi, *Int. J. Nanomedicine*, 2022, **17**, 299–331.
- 6 S. Asher and R. Priefer, *Life Sci.*, 2022, **306**, 120861.
- 7 H. Zhang, W. Wei, M. Zhao, L. Ma, X. Jiang, H. Pei, Y. Cao and H. Li, *Int. J. Biol. Sci.*, 2021, **17**, 2181.
- 8 A. E. Alkhalifa, O. Alkhalifa, I. Durdanovic, D. R. Ibrahim and S. Maragkou, *J. Dement. Alzheimer's Dis.*, 2025, **2**, 17.
- 9 F. Fereidooni, G. Komeili, H. Fanaei, T. Safari, S. Khorrami and A. K. Feizabad, *Neurol. Psychiatry Brain Res.*, 2020, **37**, 116.
- 10 M. S. Mahdy, R. H. AL-Mosawi and S. S. Hammoud, *Hilla Univ. Coll. J. Med. Sci.*, 2024, **2**, 58.
- 11 P. Kamila, K. Kar, S. Chowdhury, P. Chakraborty, R. Dutta, S. S. A. Singh S and B. G.



- Prajapati, *IBRO Neurosci. Reports*, 2025, **18**, 771.
- 12 S. Thakur, R. Dhapola, P. Sarma, B. Medhi and D. H. K. Reddy, *Inflammation*, 2023, **46**, 1.
- 13 L. Wang, Y. L. Yin, X. Z. Liu, P. Shen, Y. G. Zheng, X. R. Lan, C. B. Lu and J. Z. Wang, *Transl. Neurodegener.*, 2020, **9**, 10.
- 14 K. Khurana and N. Jaggi, *Plasmonics*, 2021, **16**, 981.
- 15 L. Wang, M. Hasanzadeh Kafshgari and M. Meunier, *Adv. Funct. Mater.*, 2020, **30**, 2005400.
- 16 Z. Ma, J. Mohapatra, K. Wei, J. P. Liu and S. Sun, *Chem. Rev.*, 2021, **123**, 3904.
- 17 K. Biaľas, D. Moschou, F. Marken and P. Estrela, *Microchim. Acta*, 2022, **189**, 172.
- 18 L. K. Sannegowda, in *Handbook of Nanomaterials for Sensing Applications*, eds. C. M. Hussain and S. K. B. T.-H. of N. for S. A. Kailasa, Elsevier, 2021, pp. 589.
- 19 N. Joudeh and D. Linke, *J. Nanobiotechnology*, 2022, **20**, 262.
- 20 J. Sidhic, M. K. Aswathi, A. Prasad, A. Tom, P. Mohan, P. Sarbadhikary, A. Narayanankutty, S. George, H. Abrahamse and B. P. George, *J. Drug Deliv. Sci. Technol.*, 2025, **105**, 106622.
- 21 S. Liu, X. Jin, Y. Ge, J. Dong, X. Liu, X. Pei, P. Wang, B. Wang, Y. Chang and X. A. Yu, *J. Nanobiotechnology*, 2025, **23**, 382.
- 22 L. Yang, J. Sun, W. Xie, Y. Liu and J. Liu, *J. Mater. Chem. B*, 2017, **5**, 5954.
- 23 B. Pancholi, M. K. Choudhary, M. Kumar, R. Babu, L. K. Vora, D. K. Khatri and D.



- Garabadu, *J. Drug Deliv. Sci. Technol.*, 2025, **107**, 106816.
- 24 M. Mahmoudi, M. P. Landry, A. Moore and R. Coreas, *Nat. Rev. Mater.*, 2023, **8**, 422.
- 25 N. M. La-Beck, M. R. Islam and M. M. Markiewski, *Front. Immunol.*, 2021, **11**, 603039.
- 26 L. Xuan, Z. Ju, M. Skonieczna, P. K. Zhou and R. Huang, *MedComm*, 2023, **4**, e327.
- 27 A. Naskar, S. Kilari, G. Baranwal, J. Kane and S. Misra, *Bioengineering*, 2024, **11**, 1222.
- 28 Y. Chen, C. Zhang, Y. Huang, Y. Ma, Q. Song, H. Chen, G. Jiang and X. Gao, *Adv. Drug Deliv. Rev.*, 2024, **207**, 115196.
- 29 S. Khorrami, A. Zarrabi, M. Khaleghi, M. Danaei and M. Mozafari, *Int. J. Nanomedicine*, 2018, **13**, 8013.
- 30 S. Khorrami, M. Dogani, S. E. Mahani, M. M. Moghaddam and R. A. Taheri, *Sci. Rep.*, 2023, **1**.
- 31 A. García-García, S. Rojas and A. Rodríguez-Diéguez, *J. Mater. Chem. B*, 2023, **11**, 7024.
- 32 X. Yi, H. Chen, Y. He and J. Wang, *J. Anal. Test.*, 2024, **8**, 251.
- 33 A. Tapia-Arellano, P. Cabrera, E. Cortés-Adasme, A. Riveros, N. Hassan and M. J. Kogan, *J. Nanobiotechnology*, 2024, **22**, 248.
- 34 J. Wang, X. Lu and Y. He, *Biosensors*, 2025, **15**, 85.
- 35 L. Agnello, C. M. Gambino, A. M. Ciaccio, F. Cacciabauda, D. Massa, A. Masucci, M. Tamburello, R. Vassallo, M. Midiri, C. Scazzone and M. Ciaccio, *Curr. Issues Mol. Biol.*, 2025, **47**, 580.
- 36 A. Abelein, *Acc. Chem. Res.*, 2023, **56**, 2653.



- 37 J. H. Kang, M. Korecka, E. B. Lee, K. A. Q. Cousins, T. F. Tropea, A. A. Chen-Plotkin, D. J. Irwin, D. Wolk, M. Brylska, Y. Wan and L. M. Shaw, *Clin. Chem.*, 2023, **69**, 1247.
- 38 J. Wang, C. Jin, J. Zhou, R. Zhou, M. Tian, H. J. Lee and H. Zhang, *Eur. J. Nucl. Med. Mol. Imaging*, 2023, **50**, 765.
- 39 M. M. Zeineh, Y. Chen, H. H. Kitzler, R. Hammond, H. Vogel and B. K. Rutt, *Neurobiol. Aging*, 2015, **36**, 2483–2500.
- 40 D. Baldaranov, V. Garcia, G. Miller, M. C. Donohue, L. M. Shaw, M. Weiner, R. C. Petersen, P. Aisen, R. Raman and M. S. Rafii, *Alzheimer's Dement. Diagnosis, Assess. Dis. Monit.*, 2023, **15**, e12431.
- 41 S. Mangalore, S. Peer and A. K. Gupta, *Asian J. Psychiatr.*, 2022, **73**, 103094.
- 42 B. T. Murti, A. D. Putri, Y. J. Huang, S. M. Wei, C. W. Peng and P. K. Yang, *RSC Adv.*, 2021, **11**, 20403.
- 43 M. Dhauria, R. Mondal, S. Deb, G. Shome, D. Chowdhury, S. Sarkar and J. Benito-León, *Int. J. Mol. Sci.*, DOI:10.3390/ijms252010911.
- 44 S. Salloway, C. Rowe and J. M. Burns, *Jama*, 2024, **332**, 1240.
- 45 X. Zhu, N. Zhang, Y. Zhang, B. Liu, Z. Chang, Y. Zhou, Y. Hao, B. Ye and M. Xu, *Anal. Methods*, 2018, **10**, 641.
- 46 Y. Zhou, H. Dong, L. Liu and M. Xu, *Small*, 2015, **11**, 2144.
- 47 F. T. C. Moreira, B. P. Correia, M. P. Sousa and G. F. Sales, *Microchim. Acta*, 2021, **188**, 334.



- 48 A. Neely, C. Perry, B. Varisli, A. K. Singh, T. Arbneshi, D. Senapati, J. R. Kalluri and P. C. Ray, *ACS Nano*, 2009, **3**, 2834.
- 49 A. C. Alguno, R. Y. Capangpangan, G. G. Dumancas, A. A. Lubguban, R. M. Malaluan and R. B. P. Rivera, eds. A. C. Alguno, R. Y. Capangpangan, G. G. Dumancas, A. A. Lubguban, R. M. Malaluan and R. B. P. Rivera, Springer Nature Singapore, Singapore, 2025, pp. 13.
- 50 F. Gao, F. Li, J. Wang, H. Yu, X. Li, H. Chen, J. Wang, D. Qin, Y. Li, S. Liu, X. Zhang and Z. H. Wang, *Biosensors*, 2023, **13**, 880.
- 51 J. K. Yang, I. J. Hwang, M. G. Cha, H. I. Kim, D. Bin Yim, D. H. Jeong, Y. S. Lee and J. H. Kim, *Small*, 2019, **15**, 1900613.
- 52 M. P. Oyarzún, A. Tapia-Arellano, P. Cabrera, P. Jara-Guajardo and M. J. Kogan, *Sensors*, 2021, **21**, 1.
- 53 U. C. Garnaik, A. Chandra, V. K. Goel, B. Gulyás, P. Padmanabhan and S. Agarwal, *Int. J. Nanomedicine*, 2024, **19**, 8271.
- 54 C. Qi, Y. Wan and X. Zhao, *J. Transl. Med.*, 2024, **22**, 539.
- 55 F. Polli, F. Simonetti, L. Surace, M. Agostini, G. Favero, F. Mazzei and R. Zumpano, *ChemElectroChem*, 2024, **11**, e202300408.
- 56 M. Negahdary and H. Heli, *Microchim. Acta*, 2019, **186**, 766.
- 57 Q. Kong, C. Liu, Y. Zhang, Y. He, R. Zhang, Y. Wang, Q. Zhou and F. Cui, *Microchim. Acta*, 2024, **191**, 328.
- 58 C. A. Razzino, V. Serafin, M. Gamella, M. Pedrero, A. Montero-Calle, R. Barderas, M.



- Calero, A. O. Lobo, P. Yáñez-Sedeño, S. Campuzano and J. M. Pingarrón, *Biosens. Bioelectron.*, 2020, **163**, 112238.
- 59 F. Chakari-Khiavi, A. Mirzaie, B. Khalilzadeh, H. Yousefi, R. Abolhasan, A. Kamrani, R. Pourakbari, K. Shahpasand, M. Yousefi and M. R. Rashidi, *Sci. Rep.*, 2023, **13**, 16163.
- 60 M. Li, Y. Zeng, Z. Huang, L. Zhang and Y. Liu, *Biosensors*, 2023, **13**, 758.
- 61 C. Ferrag and K. Kerman, *Front. Sensors*, 2020, **1**, 583822.
- 62 M. A. Siddiqui, S. A. Khan, C. Chhabra, S. Zaidi and H. Sundus, in *Computational Intelligence Algorithms for the Diagnosis of Neurological Disorders*, CRC Press, 2025, pp. 69.
- 63 R. Lapusan, R. Borlan and M. Focsan, *Nanoscale Adv.*, 2024, **6**, 2234.
- 64 S. Luo, C. Ma, M.-Q. Zhu, W.-N. Ju, Y. Yang and X. Wang, *Front. Cell. Neurosci.*, 2020, **14**, 21.
- 65 J. Zeng, J. Wu, M. Li and P. Wang, *Arch. Med. Res.*, 2018, **49**, 282.
- 66 M. Plissonneau, J. Pansieri, L. Heinrich-Balard, J. F. Morfin, N. Stransky-Heilkron, P. Rivory, P. Mowat, M. Dumoulin, R. Cohen, É. Allémann, É. Tóth, M. J. Saraiva, C. Louis, O. Tillement, V. Forge, F. Lux and C. Marquette, *J. Nanobiotechnology*, 2016, **14**, 60.
- 67 Y. Liang, T. Zhang and M. Tang, *J. Appl. Toxicol.*, 2022, **42**, 17.
- 68 P. J. Withers, C. Bouman, S. Carmignato, V. Cnudde, D. Grimaldi, C. K. Hagen, E. Maire, M. Manley, A. Du Plessis and S. R. Stock, *Nat. Rev. Methods Prim.*, 2021, **1**, 18.



- 69 I. Mutreja, N. Maalej, A. Kaushik, D. Kumar and A. Raja, *Mater. Adv.*, 2023, **4**, 3967.
- 70 O. Betzer, M. Shilo, R. Opoichinsky, E. Barnoy, M. Motiei, E. Okun, G. Yadid and R. Popovtzer, *Nanomedicine*, 2017, **12**, 1533.
- 71 S. Sivanesan and S. Rajeshkumar, in *Nanobiotechnology in Neurodegenerative Diseases*, eds. M. Rai and A. Yadav, Springer International Publishing, Cham, 2019, pp. 289.
- 72 D. Tripathi, M. Hardaniya, S. Pande and D. Maity, *J. Imaging*, 2025, **11**, 87.
- 73 P. Jara-Guajardo, P. Cabrera, F. Celis, M. Soler, I. Berlanga, N. Parra-Muñoz, G. Acosta, F. Albericio, F. Guzman, M. Campos, A. Alvarez, F. Morales-Zavala and M. J. Kogan, *Nanomaterials*, 2020, **10**, 690.
- 74 B. Dunn, M. Hanafi, J. Hummel, J. R. Cressman, R. Veneziano and P. V. Chitnis, *Bioengineering*, 2023, **10**, 954.
- 75 J. Jang, Y. Jo and C. B. Park, *ACS Nano*, 2022, **16**, 18515.
- 76 S. J. Zhong, K. Y. Chen, S. L. Wang, F. Manshahi, N. Jing, K. D. Wang, S. C. Liu and Y. L. Zhou, *Rare Met.*, 2024, **43**, 6233.
- 77 M. A. Subhan, N. Neogi, K. P. Choudhury and M. M. Rahman, *Chemosensors*, 2025, **13**, 49.
- 78 B. Sharma and K. Pervushin, *Magnetochemistry*, 2020, **6**, 1.
- 79 Y. Zhan, R. Fei, Y. Lu, Y. Wan, X. Wu, J. Dong, D. Meng, Q. Ge and X. Zhao, *Analyst*, 2022, **147**, 4124.
- 80 X. Zhang, S. Liu, X. Song, H. Wang, J. Wang, Y. Wang, J. Huang and J. Yu, *ACS*



- Sensors*, 2019, **4**, 2140.
- 81 M. H. Stenzel, *Angew. Chemie - Int. Ed.*, 2021, **60**, 2202.
- 82 A. Taheri-Kafrani, H. Shirzadfar, A. Abbasi Kajani, B. K. Kudhair, L. Jasim Mohammed, S. Mohammadi and F. Lotfi, *J. Biotechnol.*, 2021, **331**, 26.
- 83 C. Li, N. Wang, G. Zheng and L. Yang, *ACS Appl. Mater. Interfaces*, 2021, **13**, 46406.
- 84 Y. Sattar, *Glob. J. Pharm. Pharm. Sci.*, 2018, **6**, 6.
- 85 S. Katebi, A. Esmaeili, K. Ghaedi and A. Zarrabi, *Int. J. Nanomedicine*, 2019, **14**, 2157.
- 86 X. ge Liu, L. Zhang, S. Lu, D. qun Liu, Y. ru Huang, J. Zhu, W. wei Zhou, X. lin Yu and R. tian Liu, *J. Nanobiotechnology*, 2020, **18**, 160.
- 87 H. Zhou, Y. Gong, Y. Liu, A. Huang, X. Zhu, J. Liu, G. Yuan, L. Zhang, J. an Wei and J. Liu, *Biomaterials*, 2020, **237**, 119822.
- 88 Y. Liu, Y. Chen, Y. Gong, H. Yang and J. Liu, *ACS Appl. Nano Mater.*, 2023, **6**, 5384.
- 89 M. Srinivasan, M. Rajabi and S. A. Mousa, *Nanomaterials*, 2015, **5**, 1690.
- 90 M. C. Chiang, Y. P. Yang, C. J. B. Nicol and C. J. Wang, *Int. J. Mol. Sci.*, 2024, **25**, 2360.
- 91 X. Zhang, Y. Li and Y. Hu, *Colloids Surfaces A Physicochem. Eng. Asp.*, 2020, **605**, 125288.
- 92 Y. Hu, H. Guo, S. Cheng, J. Sun, J. Du, X. Liu, Y. Xiong, L. Chen, C. Liu, C. Wu and H. Tian, *Int. J. Nanomedicine*, 2023, **18**, 6797.
- 93 Y. Guan, N. Gao, J. Ren and X. Qu, *Chem. - A Eur. J.*, 2016, **22**, 14523.



- 94 H. Amani, R. Habibey, F. Shokri, S. J. Hajmiresmail, O. Akhavan, A. Mashaghi and H. Pazoki-Toroudi, *Sci. Rep.*, 2019, **9**, 6044.
- 95 F. Gao, J. Zhao, P. Liu, D. Ji, L. Zhang, M. Zhang, Y. Li and Y. Xiao, *Int. J. Biol. Macromol.*, 2020, **142**, 265.
- 96 A. M. Almehdi, D. H. Aboubaker, R. Hamdy and A. El-Keblawy, *Toxicol. Reports*, 2025, **14**, 101906.
- 97 A. Vilella, D. Belletti, A. K. Sauer, S. Hagemeyer, T. Sarowar, M. Masoni, N. Stasiak, J. J. E. Mulvihill, B. Ruozi, F. Forni, M. A. Vandelli, G. Tosi, M. Zoli and A. M. Grabrucker, *J. Trace Elem. Med. Biol.*, 2018, **49**, 210.
- 98 S. S. El-Hawwary, H. M. Abd Almaksoud, F. R. Saber, H. Elimam, A. M. Sayed, M. A. El Raey and U. R. Abdelmohsen, *RSC Adv.*, 2021, **11**, 18009.
- 99 L. Yang, Q. Chen, Y. Liu, J. Zhang, D. Sun, Y. Zhou and J. Liu, *J. Mater. Chem. B*, 2014, **2**, 1977.
- 100 Y. Chen, J. an Wei, L. Wang, Q. Cai, F. Yang, L. Zhang, J. Liu and Y. Liu, *Chem. Eng. J.*, 2024, **492**, 151868.
- 101 A. Sabu, Y. C. Huang, R. Sharmila, C. Y. Sun, M. Y. Shen and H. C. Chiu, *Mater. Today Bio*, 2024, **28**, 101213.
- 102 S. Pawar, M. A. Rauf, H. Abdelhady and A. K. Iyer, *Exploration*, 2025, **5**, 20230137.
- 103 F. Zeng, K. Peng, L. Han and J. Yang, *ACS Biomater. Sci. Eng.*, 2021, **7**, 3573.
- 104 R. C. Triulzi, Q. Dai, J. Zou, R. M. Leblanc, Q. Gu, J. Orbulescu and Q. Huo, *Colloids Surfaces B Biointerfaces*, 2008, **63**, 200–208.



- 105 D. Lin, R. He, S. Li, Y. Xu, J. Wang, G. Wei, M. Ji and X. Yang, *ACS Chem. Neurosci.*, 2016, **7**, 1728.
- 106 E. Okła, P. Białecki, M. Kędzierska, E. Pędziwiatr-Werbicka, K. Miłowska, S. Takvor, R. Gómez, F. J. de la Mata, M. Bryszewska and M. Ionov, *Int. J. Mol. Sci.*, 2023, **24**, 6638.
- 107 N. Lopez-Barbosa, J. G. Garcia, J. Cifuentes, L. M. Castro, F. Vargas, C. Ostos, G. P. Cardona-Gomez, A. M. Hernandez and J. C. Cruz, *Drug Deliv.*, 2020, **27**, 864.
- 108 X. Ding, Y. Hu, X. Feng, Z. Wang, Q. Song, C. Dai, B. Yang, X. Fu, D. Sun and C. Fan, *Exploration*, 2025, **5**, e20230178.
- 109 L. Zhao, T. Peng and S. Y. Wu, ed. M. M. Rahman, IntechOpen, Rijeka, 2025.
- 110 G. Wang, X. Shen, X. Song, N. Wang, X. Wo and Y. Gao, *Neurotoxicology*, 2023, **95**, 12.
- 111 V. Sundararajan, G. D. Venkatasubbu and S. Sheik Mohideen, *3 Biotech*, 2021, **11**, 159.
- 112 K. A. Youssif, E. G. Haggag, A. M. Elshamy, M. A. Rabeh, N. M. Gabr, A. Seleem, M. Alaraby Salem, A. S. Hussein, M. Krischke, M. J. Mueller and U. R. Abdelmohsen, *PLoS One*, 2019, **14**, e0223781.
- 113 R. Ceylan, A. Demirbas, I. Ocsoy and A. Aktumsek, *Sustain. Chem. Pharm.*, 2021, **21**, 100426.
- 114 N. dos Santos Tramontin, S. da Silva, R. Arruda, K. S. Ugioni, P. B. Canteiro, G. de Bem Silveira, C. Mendes, P. C. L. Silveira and A. P. Muller, *Mol. Neurobiol.*, 2020, **57**, 926.
- 115 N. Suganthy, V. Sri Ramkumar, A. Pugazhendhi, G. Benelli and G. Archunan, *Environ. Sci. Pollut. Res.*, 2018, **25**, 10418.



- 116 B. G. Anand, Q. Wu, G. Karthivashan, K. P. Shejale, S. Amidian, H. Wille and S. Kar, *Bioact. Mater.*, 2021, **6**, 4491.
- 117 K. Hou, J. Zhao, H. Wang, B. Li, K. Li, X. Shi, K. Wan, J. Ai, J. Lv, D. Wang, Q. Huang, H. Wang, Q. Cao, S. Liu and Z. Tang, *Nat. Commun.*, 2020, **11**, 4790.
- 118 T. Yin, W. Xie, J. Sun, L. Yang and J. Liu, *ACS Appl. Mater. Interfaces*, 2016, **8**, 19291–19302.
- 119 M. J. Kim, S. U. Rehman, F. U. Amin and M. O. Kim, *Nanomedicine Nanotechnology, Biol. Med.*, 2017, **13**, 2533.
- 120 X. Huo, Y. Zhang, X. Jin, Y. Li and L. Zhang, *J. Photochem. Photobiol. B Biol.*, 2019, **190**, 98.
- 121 O. A. R. Abozaid, M. W. Sallam, S. El-Sonbaty, S. Aziza, B. Emad and E. S. A. Ahmed, *Biol. Trace Elem. Res.*, 2022, **200**, 5104–5114.
- 122 B. Gholamigeravand, S. Shahidi, S. Afshar, P. Gholipour, A. Samzadeh-kermani, K. Amiri, M. Majidi, R. Abbasalipourkabir, M. R. Arabestani and S. Soleimani Asl, *Life Sci.*, 2021, **272**, 119246.
- 123 J. Zhang, X. Zhou, Q. Yu, L. Yang, D. Sun, Y. Zhou and J. Liu, *ACS Appl. Mater. Interfaces*, 2014, **6**, 8475.
- 124 T. Yin, L. Yang, Y. Liu, X. Zhou, J. Sun and J. Liu, *Acta Biomater.*, 2015, **25**, 172–183.
- 125 X. Yuan, Z. Jia, J. Li, Y. Liu, Y. Huang, Y. Gong, X. Guo, X. Chen, J. Cen and J. Liu, *J. Mater. Chem. B*, 2021, **9**, 7835.
- 126 M. H. Ahmed, J. A. Byrne and T. E. Keyes, *Mater. Sci. Eng. C*, 2014, **39**, 227–234.



- 127 M. Sanati, S. Aminyavari, F. Khodaghali, M. J. Hajipour, P. Sadeghi, M. Noruzi, A. Moshtagh, H. Behmadi and M. Sharifzadeh, *Neurotoxicology*, 2021, **85**, 145.
- 128 M. Glat, H. Skaat, N. Menkes-Caspi, S. Margel and E. A. Stern, *J. Nanobiotechnology*, 2013, **11**, 32.
- 129 H. J. Kwon, M. Y. Cha, D. Kim, D. K. Kim, M. Soh, K. Shin, T. Hyeon and I. Mook-Jung, *ACS Nano*, 2016, **10**, 2860.
- 130 N. Ahmed, H. Fessi and A. Elaissari, *Drug Discov. Today*, 2012, **17**, 928.
- 131 C. Zhou, F. Zeng, H. Yang, Z. Liang, G. Xu, X. Li, X. Liu and J. Yang, *Eur. J. Nucl. Med. Mol. Imaging*, 2024, **51**, 2953.
- 132 M. Shahalaei, A. K. Azad, W. M. A. W. Sulaiman, A. Derakhshani, E. B. Mofakham, M. Mallandrich, V. Kumarasamy and V. Subramaniyan, *Front. Chem.*, 2024, **12**, 1398979.
- 133 J. Jia, S. Zhao, J. Zhao and Y. Gao, *Front. Pharmacol.*, 2025, **16**, 1510798.
- 134 S. N. Mir Najib Ullah, O. Afzal, A. S. A. Altamimi, H. Ather, S. Sultana, W. H. Almalki, P. Bharti, A. Sahoo, K. Dwivedi, G. Khan, S. Sultana, A. Alzahrani and M. Rahman, *Biomedicines*, 2023, **11**, 1752.
- 135 A. Vijayan, B. S. Sivamaruthi, P. Kesika, N. Sisubalan and C. Chaiyasut, in *Nanotechnology in the Life Sciences*, eds. B. S. Sivamaruthi, N. Sisubalan, P. Kesika and K. Varaprasad, Springer Nature Switzerland, Cham, 2025, vol. Part F98, pp. 203.
- 136 F. Morales-Zavala, P. Jara-Guajardo, D. Chamorro, A. L. Riveros, A. Chandia-Cristi, N. Salgado, P. Pismante, E. Giralt, M. Sánchez-Navarro, E. Araya, R. Vasquez, G. Acosta, F. Albericio, A. Alvarez R and M. J. Kogan, *Biomater. Sci.*, 2021, **9**, 4178.



- 137 D. Huang, Q. Wang, Y. Cao, H. Yang, M. Li, F. Wu, Y. Zhang, G. Chen and Q. Wang, *ACS Nano*, 2023, **17**, 5033.
- 138 L. W. Ribeiro, M. Pietri, H. Ardila-Osorio, A. Baudry, F. Boudet-Devaud, C. Bizingre, Z. E. Arellano-Anaya, A. M. Haeberlé, N. Gadot, S. Boland, S. Devineau, Y. Bailly, O. Kellermann, A. Bencsik and B. Schneider, *Part. Fibre Toxicol.*, 2022, **19**, 48.
- 139 N. J. Siddiqi, M. A. K. Abdelhalim, A. K. El-Ansary, A. S. Alhomida and W. Y. Ong, *J. Neuroinflammation*, 2012, **9**, 123.
- 140 M. H. Fathian-Nasab, M. A. Manavi, M. Gelivarisarshari, S. M. Daghighi, C. Beyer, M. Baeeri and N. Sanadgol, *Colloids Surfaces B Biointerfaces*, 2025, **255**, 114909.
- 141 D. V. Kladko, A. S. Falchevskaya, N. S. Serov and A. Y. Prilepskii, *Int. J. Mol. Sci.*, 2021, **22**, 5266.
- 142 W. Zhang, R. Taheri-Ledari, F. Ganjali, S. S. Mirmohammadi, F. S. Qazi, M. Saeidirad, A. KashtiAray, S. Zarei-Shokat, Y. Tian and A. Maleki, *RSC Adv.*, 2022, **13**, 80.
- 143 M. Barbalinardo, J. Bertacchini, L. Bergamini, M. S. Magarò, L. Ortolani, A. Sanson, C. Palumbo, M. Cavallini and D. Gentili, *Nanoscale*, 2021, **13**, 14119.
- 144 K. Xiao, Y. Li, J. Luo, J. S. Lee, W. Xiao, A. M. Gonik, R. G. Agarwal and K. S. Lam, *Biomaterials*, 2011, **32**, 3435.
- 145 X. Bai, S. Wang, X. Yan, H. Zhou, J. Zhan, S. Liu, V. K. Sharma, G. Jiang, H. Zhu and B. Yan, *ACS Nano*, 2020, **14**, 289.
- 146 J. Liu, Z. Liu, Y. Pang and H. Zhou, *J. Nanobiotechnology*, 2022, **20**, 127.
- 147 Y. H. Luo, L. W. Chang and P. Lin, *Biomed Res. Int.*, 2015, **2015**, 143720.



- 148 M. Alaei, K. Koushki, K. Taebi, M. Yousefi Taba, S. Keshavarz Hedayati and S. Keshavarz Shahbaz, *RSC Adv.*, 2025, **15**, 5426.
- 149 J. S. Suk, Q. Xu, N. Kim, J. Hanes and L. M. Ensign, *Adv. Drug Deliv. Rev.*, 2016, **99**, 28.
- 150 V. S. Guido, P. H. Olivieri, M. L. Brito, B. C. Prezoto, D. S. T. Martinez, M. L. V. Oliva and A. A. Sousa, *Langmuir*, 2024, **40**, 12167.
- 151 J. Liu, D. A. Sonshine, S. Shervani and R. H. Hurt, *ACS Nano*, 2010, **4**, 6903.
- 152 Ł. Niżnik, M. Noga, D. Kobylarz, A. Frydrych, A. Krośniak, L. Kapka-Skrzypczak and K. Jurowski, *Int. J. Mol. Sci.*, 2024, **25**, 4057.
- 153 L. V. Kiss, Z. Sávoly, A. Ács, A. Seres and P. I. Nagy, *Environ. Sci. Pollut. Res.*, 2021, **28**, 34436.
- 154 X. Ge, Z. Cao and L. Chu, *Antioxidants*, 2022, **11**, 791.
- 155 S. Ahmad, S. Ahmad, S. Ali, M. Esa, A. Khan and H. Yan, *Int. J. Nanomedicine*, 2024, **19**, 3187.



## Data availability statements

No primary research results, software or code have been included and no new data were generated or analysed as part of this review.

